Graduate School ETD Form 9
(Revised 01/14)

PURDUE UNIVERSITY
GRADUATE SCHOOL
Thesis/Dissertation Acceptance

This is to certify that the thesis/dissertation prepared

By Selene Hernandez-Buquer

Entitled
CHARACTERIZATION OF A FATTY ACID ELONGASE CONDENSING ENZYME BY SITE-DIRECTED MUTAGENESIS AND BIOCHEMICAL ANALYSIS

For the degree of Master of Science

Is approved by the final examining committee:

Eric Long

Brenda Blacklock

Lei Li

To the best of my knowledge and as understood by the student in the *Thesis/Dissertation Agreement. Publication Delay, and Certification/Disclaimer (Graduate School Form 32)*, this thesis/dissertation adheres to the provisions of Purdue University's "Policy on Integrity in Research" and the use of copyrighted material.

Brenda Blacklock

Approved by Major Professor(s): _____

_____

Approved by: Eric Long 03/14/2014

Head of the Department Graduate Program Date

CHARACTERIZATION OF A FATTY ACID ELONGASE CONDENSING ENZYME BY SITE-DIRECTED MUTAGENESIS AND BIOCHEMICAL ANALYSIS

A Thesis

Submitted to the Faculty

of

Purdue University

by

Selene Hernandez Buquer

In Partial Fulfillment of the

Requirements for the Degree

of

Master of Science

May 2014

Purdue University

Indianapolis, Indiana

Este trabajo esta dedicado a mis padres, a quien les agradezco todo su apoyo y su esfuerzo. Les dedico cada palabra ya que ellos sacrificaron todo para darme la mejor oportunidad de crecer como individuo y profesional. Les agradezco a mis abuelos por ser mis segundos padres, por quererme y apoyarme sin importar la distancia. Gracias.

ACKNOWLEDGEMENTS

I am very thankful to all the individuals in the Chemistry and Chemical Biology Department at IUPUI that encouraged and helped me to successfully complete my graduate degree. I am very appreciative of my advisor Dr. Brenda Blacklock for her support, guidance and giving me the opportunity to work by her side. I would also like to thank my committee members for their patience and direction during the completion of my degree. I would like to thank my peers and fellow lab members for their support.

I would like to thank Miami University Center for Bioinformatics and Functional Genomics for their help on DNA sequencing and Martin Bard, IUPUI for the Erg27 loading control used in these experiments.

TABLE OF CONTENTS

LIST OF TABLES

Table Page

LIST OF FIGURES

ABBREVIATIONS

AA	arachidonic acid
Acc1	acetyl-CoA carboxylase
ACP	acyl-carrier protein
ALD	adrenoleukodystrophy
Asn	asparagine
CMC	critical micelle concentration
CoA	coenzyme A
Cys	cysteine
*Dpn*l	*Diplococcus pneumonia* G41 enzyme
EDTA	ethylenediaminetetraacedic acid
ELO	elongase
EloA	elongase A
EPA	eicosapentaenoic acid
Erg27	ergosterol
EV	empty vector
FAME (s)	fatty acid methyl ester (s)
FAS	fatty acid synthase
GC/MS	gas chromatography-mass spectrometry
His	histidine
HOS3	high expression of osmotically responsive genes
IgG	immunoglobulin G
KCS	3-ketoacyl CoA synthase
kDa	kiloDalton
LB	luria broth
LC	loading control
LiAc	lithium acetate
MAT	malonyl-CoA-ACP transacylase
MUFA	monounsaturated fatty acid
NADPH	nicotinamide adenine dinucleotide phosphate
OD	opotimal density
PAGE	polyacrylamide gel electrophoresis
PCR	polymerase chain reaction
PEG	polyethylene glycol
PES1	PUFA specific elongase
PUFA	polyunsaturated fatty acid
SDS	sodium dodecyl sulfate
SFA	saturated fatty acid
SOC	super optimal broth

TIC	total ion chromatogram
TTBS	tris-buffered saline with tween 20
VLCFA(s)	very long chain fatty acid (s)
YPAD	yeast extract-peptone-dextrose plus adenine

ABSTRACT

Hernandez Buquer, Selene. M.S., Purdue University, May 2014 Characterization of Fatty Acid Elongase Condensing Enzyme by Site-Directed Mutagenesis and Biochemical Analysis. Major Professor: Brenda Blacklock.

Fatty acid elongation is the extension of *de novo* synthesized fatty acids through a series of four reactions analogous to those of fatty acid synthase. ELOs catalyze the first reaction in the elongation pathway through the condensation of an acyl group with a two-carbon unit derived from malonyl-CoA. This study uses the condensing enzyme, EloA, from the cellular slime mold, *Dictyostelium discoideum* as a model for the family of ELOs. EloA has substrate specificity for monounsaturated and saturated C_{16} fatty acids and catalyzes the elongation of $16{:}1^{\triangle 9}$ to $18{:}1^{\triangle 11}$. Site-directed mutagenesis was used to change residues highly conserved among the ELO family to examine their potential role in the condensation reaction. Mutant EloAs were expressed in yeast and fatty acid methyl esters prepared from total cellular lipids were analyzed by gas chromatography/mass spectrometry. Sixteen out of twenty mutants had a decrease in $18{:}1^{\Delta 11}$ production when compared to the wild-type EloA with little to no activity observed in ten mutants, four mutants had within 20% of wild-type activity, and six mutants had 10-60% of wild-type activity. Immunoblot studies using anti-EloA serum were used to determine if the differences in elongation activity were related to changes in protein expression for each mutant. Analysis of immunoblots indicated that those mutants with little to no activity, with the exception of T130A and Q203A, had

comparable protein expression to the wild-type. Further research included the solubilization of the His_6-ELoA fusion protein and preliminary work toward the isolation of the tagged protein and the use of a radiolabeled condensation assay to determine the activity of the eluted protein. Preliminary results indicated that the protein was solubilized but the eluted protein showed no activity when examined by a condensation assay. The work presented here contributes to a better understanding of the role of certain amino acid residues in the activity of EloA and serves as a stepping-stone for future EloA isolation work.

CHAPTER 1. INTRODUCTION

1.1 Lipids and Very Long-Chain Fatty Acids

Lipids are structurally diverse and serve many biological functions such as the formation of the cellular membrane, regulation of the fluidity of the lipid bilayer, signal transduction and energy storage. Lipids are classified as fatty acids, sterols, oils, and sphingolipids among others (1). The structural diversity of lipids allows for different roles in biochemical processes. For example, the myelin sheath that surrounds the axons in nerve cells are rich in sphingomyelin (2). Additionally, lipids affect protein structure and activity thus affecting cellular function; protein function is affected by protein-lipid interactions, which depend on factors such as chain length, degree of unsaturation, and backbone structure among others (1). Overall, the chemical and physical properties of lipids allow them to be involved at many levels of cellular function.

Many lipids are classified as long-chain fatty acids depending on their chain lengths. Very long-chain fatty acids (VLCFA) have chain lengths of C_{18} and greater and play pivotal intracellular roles such as maintaining cellular structure and regulation and extracellular roles such as cuticular wax formation and energy storage. The acyl chains of ceramides and more complex sphingolipids, the building blocks of membrane microdomains, are often VLCFAs (3).

VLCFAs are thought to stabilize curved membranes by being present in both leaflets of the lipid bilayer as well as aiding with the maintenance and function of the nuclear envelope (4). Structurally, VLCFA are classified as saturated, monounsaturated or polyunsaturated very long chain fatty acids (5) (Figure 1.1) depending upon the extent of double bond formation.

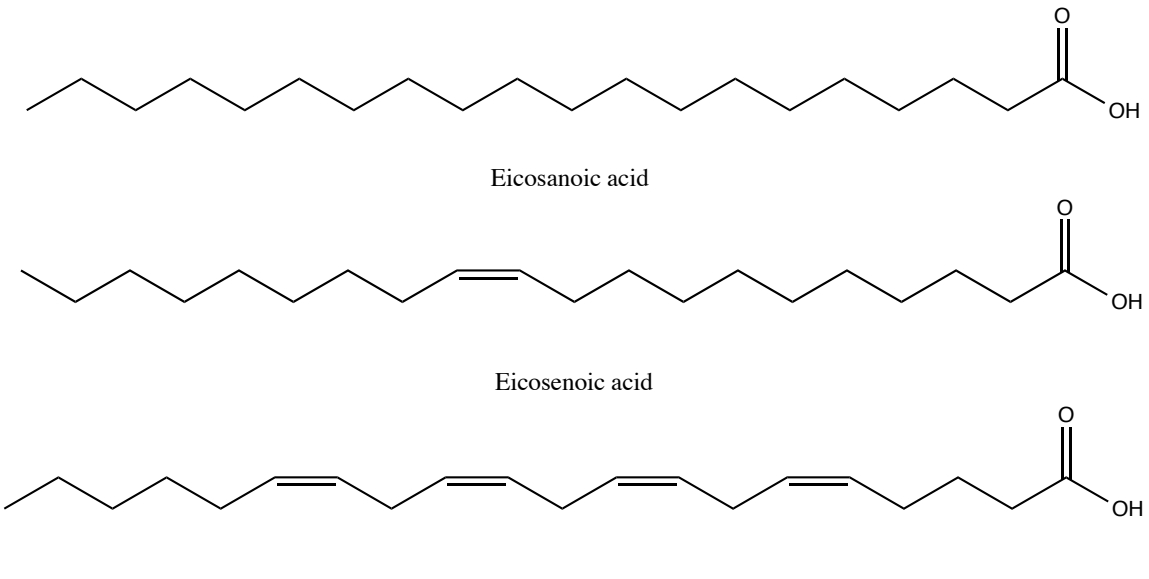

Figure 1.1. A saturated (eicosanoic acid-20:0), monounsaturated (eicosenoic acid-$20{:}1^{\Delta 11}$), and polyunsaturated (arachidonic acid-$20{:}4^{\Delta 5,8,11,14}$) VLCFA. Nomenclature is in the Δ^x format, where the x indicates the location of the double bond counting from the carboxylic acid. The number:number nomenclature represents the number of carbons:number of double bonds.

Both land plants and animals exploit the hydrophobic nature of VLCFAs for protection against dehydration and the environment. In plants, VLCFAs up to C_{32} are found as components of cuticular wax and suberin (6). Additionally, some plant seed oils contain VLCFAs that are integrated into wax esters or triacyglyerols (7).

In *Arabidopsis*, more than fifty percent of VLCFAs are key components of wax synthesis that will produce aliphatic wax components to protect plant tissue from environmental factors and disease (6). In mammals, VLCFAs longer than C_{30} are pivotal for the proper structure and function of the skin by creating a permeability barrier. C_{22} fatty acids are an important component of lipids present in the retina and both arachidonic acid (AA, $20{:}4^{\Delta 5,8,11,14}$) and eicosapentaenoic acid (EPA, $20{:}5^{\Delta 5,8,11,14,17}$) are precursors to eicosanoids which are involved in blood pressure regulation, cell signaling, blood clotting and inflammatory response (8, 9). Furthermore, studies have shown that mutation of enzymes that synthesize VLCFAs can cause diseases in humans. For example, a mutation of an elongase of very long chain fatty acids (ELOVL4), causes Stargardt disease-3, a disease leading to the accumulation of lipofuscin and central vision loss (8). In mammals, ELOVL4 is proposed to aid in the synthesis of docosahexaenoic acid which is present in the phospholipids found in the retina (8).

Although VLCFAs participate in multiple biological processes, the mechanism that gives them their diverse chain lengths is not well understood. VLCFAs are produced at the ER from *de novo* synthesized C_{16} and C_{18} fatty acids through the activity of a membrane-bound fatty acid elongase complex comprised of a condensing enzyme, two reductases, a dehydratase, and, as recently shown in plants, an immunophilin-like scaffolding protein (10).

1.1.2. Fatty Acid Synthesis

Fatty acids are essential to all organisms and are long chain carboxylic acids. Common fatty acids are those with C_{16} or C_{18} chain lengths that can be saturated or unsaturated at multiple locations. Fatty acid biosynthesis takes place in the cytosol and involves the condensation, catalyzed by fatty acid synthases, of C_2 units derived from acetate to fatty acyl groups linked to the acyl-carrier protein (ACP) to produce essential fatty acids. Fatty acid synthesis is catalyzed by either a type I system which involves a single polypeptide or a type II system that involves multiple separate polypeptides (11). Fatty acids in mammals takes place using a type I fatty acid synthase (FAS) while most bacterial and all plants use a type II system (11)

The first reaction involves the addition of CO_2 to acetyl-CoA catalyzed by acetyl-CoA carboxylase to yield malonyl-CoA, a step that requires ATP. The malonyl group is transferred to ACP as catalyzed by malonyl-CoA-ACP transacylase (MAT) to generate malonyl-ACP. Simultaneously, the acetyl group from acetyl-CoA is transferred to ACP by acetyl-CoA-ACP transacylase (2). The next step involves the condensation reaction, catalyzed by fatty acid synthase, of a C2 unit from malonyl-ACP with acetyl-ACP. Malonyl-CoA is decarboxylated resulting in the formation of a carbanion that attacks the acetyl-thioester bond in acetyl-ACP yielding 3-ketoacyl-ACP. The subsequent reactions involve reduction of the 3-ketoacyl-ACP product, which involves NADPH as the electron donor and dehydration of the 3-hydroxyacyl-ACP product where the carbonyl group is converted into an alkyl group to yield the enoyl-ACP product, which is reduced (again requiring NADPH) to a product that is two carbons longer. (Figure 1.2) (2).

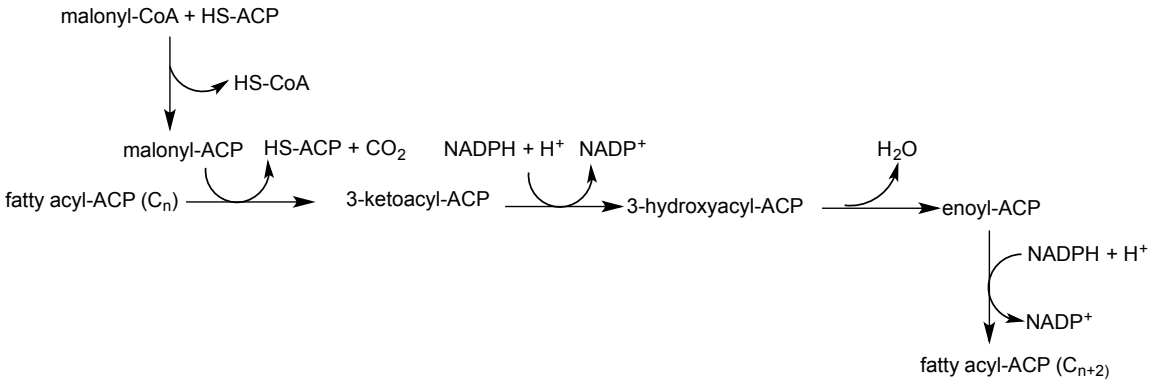

Figure 1.2. Fatty acid biosynthesis overview.

1.2 Fatty acid elongation and condensing enzymes

In comparison to cytosolic fatty acid biosynthesis, fatty acid elongation takes place in the endoplasmic reticulum where a system of enzymes catalyze the condensation of a C_2-unit from malonyl-CoA with an acyl-CoA primer (C_{16} or C_{18}) to form an elongated 3-ketoacyl-CoA, the reduction of the carbonyl group to a hydroxyl group, followed by a dehydration to form a trans alkene. The alkene is further reduced to yield a acyl-CoA product two carbons longer (12) (Figure 1.3). The elongation of fatty acids requires malonyl-CoA, a product of the carboxylation of acetyl-CoA by acetyl-CoA carboxylase (Acc1) (13). Once the malonyl-CoA, donor of two carbon units, is available the elongation process proceeds. The first step of the fatty acid elongation process is the condensation, by a condensing enzyme (KCS/ELO) of acyl-CoA with the malony-CoA unit derived from Acc1 yielding a 3-ketoacyl-CoA product.

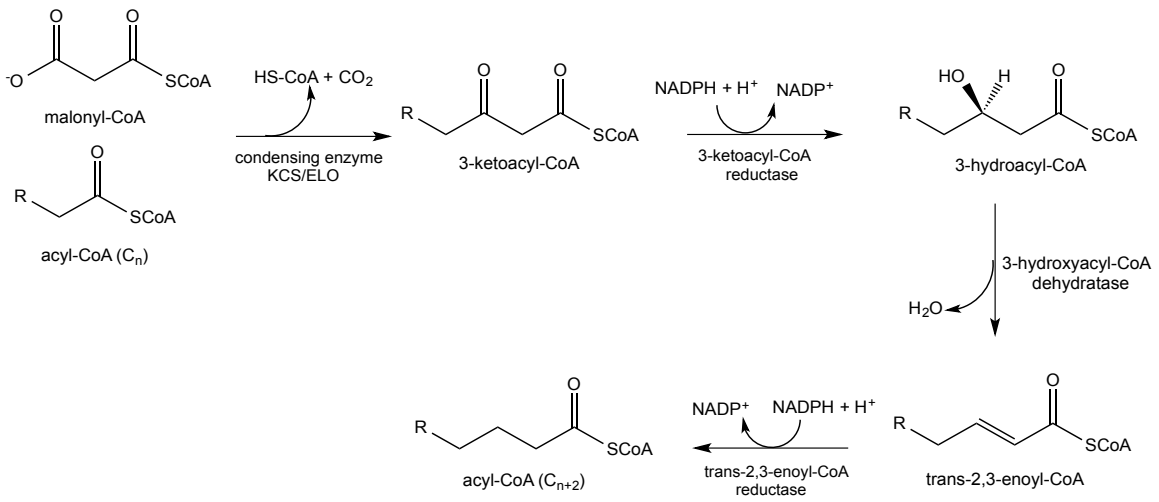

Figure 1.3. Fatty acid elongation pathway.

Two families of fatty acid elongase condensing enzymes have been described previously: the ELOs and the 3-ketoacyl-CoA synthases (KCSs) (14-16). Animals, fungi, and other higher-order eukaryotes accomplish fatty acid elongation with a distinct family of condensing enzymes, first described in *Saccharomyces cerevisiae* as ELOs, which have been modeled to span the membrane five to seven times (16-19). *Arabidopsis* has predicted homologs to the ELOs (20). In plants and protists, 3-ketoacyl-CoA synthases (KCSs) with sequence similarities to the canonical Fatty Acid Elongase 1 KCS (FAE1 KCS) catalyze the initial step in fatty acid elongation and have apparent structural and catalytic similarities with the Type II fatty acid synthase (FAS) condensing enzyme (10, 21-25).

Although ELOs and KCSs catalyze the condensation reaction with the same substrates (malonyl-CoA and acyl-CoA), they do not have topological or sequence similarities. Classical KCSs catalyze fatty acid elongation through a Claisen-like

mechanism. Sequence alignment and mutagenesis have demonstrated that FAE1 KCS possesses a catalytic triad identical to those found in fatty acid synthase and polyketide synthase condensing enzymes (Cys His His/Asn) (11, 26). These enzymes catalyze the first step in elongation (26, 27) where the acyl-CoA substrate enters the active site first and, upon a nucleophilic substitution reaction, is covalently bound by the active site cysteine releasing the CoA moiety. The malonyl-CoA substrate then enters the active site and, either in a step-wise or concerted fashion, is decarboxylated and the enolate/carbanion nucleophile formed attacks the carbonyl group of the acyl primer, generating the 3-ketoacyl CoA product via an enzyme-bound tetrahedral intermediate (11) (Figure 1.4).

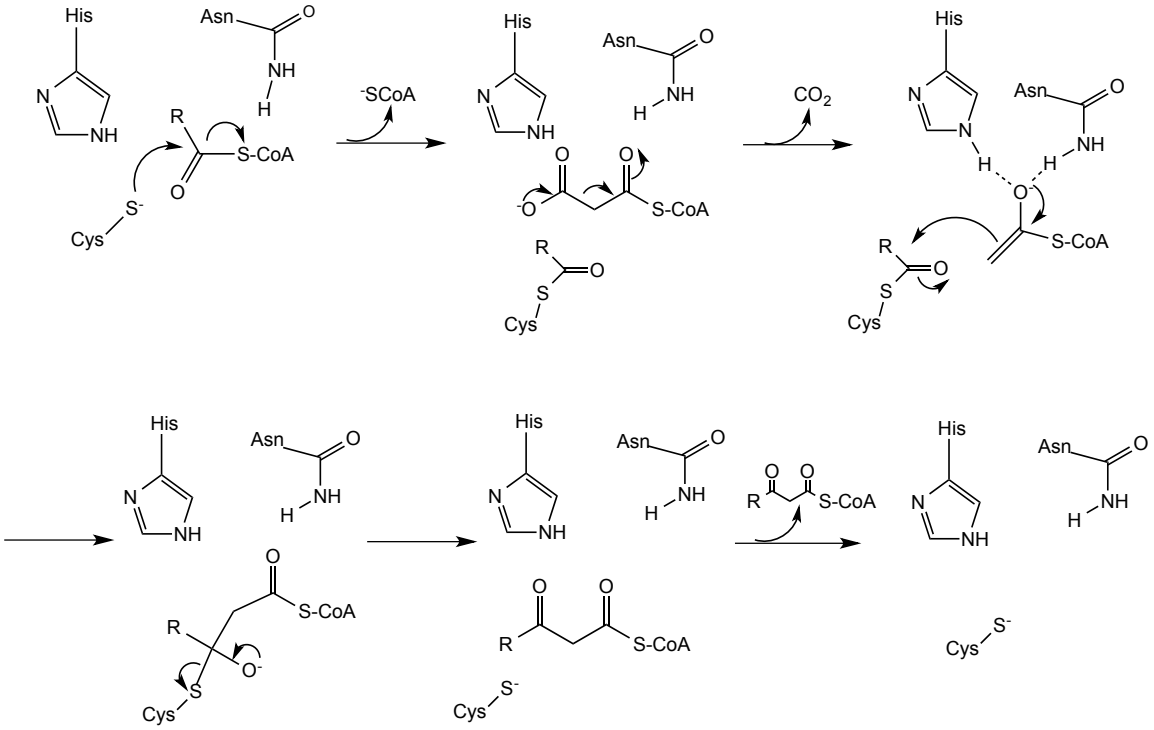

Figure 1.4. Claisen-like condensation reaction mechanism illustrating the role of the catalytic triad (Cys/His/Asn) of a condensing enzyme during fatty acid elongation.

1.2.1 ELOs: condensing enzymes

ELOs have substrate specificities that cover a wide range of fatty acid chain length and degrees of unsaturation and can be classified into phylogenetic clades based on their biochemically-characterized activity with saturated and mono- or polyunsaturated substrates (Figure 1.5) (28-30).

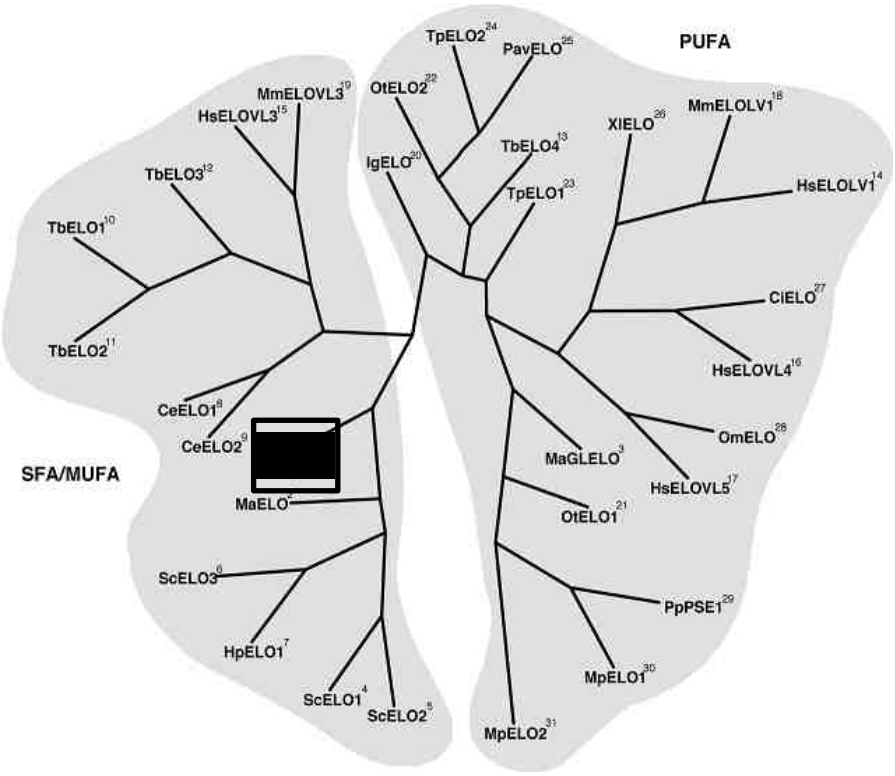

Figure 1.5. Phylogenetic tree of functionally characterized ELO family members. EloA clusters with other ELOs with substrate specificities towards MUFA/SFA.

In yeast, ELO2 and ELO3 are responsible for the production of the saturated C_{24} and C_{26} acyl chains found in sphingolipids and a simultaneous disruption of the genes encoding these ELOs is synthetically lethal (13, 16, 18). Additionally, ELO1 elongates medium and long-chain fatty acids.

Mutations in yeast ELOs demonstrate the importance of these enzymes in fatty acid elongation (13). Mutations in ELO2 lead to defects in β-glucan synthase activity, glucans are polysaccharide polymers that are major components of the cell wall in *S. cerevisiae* (31). In ELO3, mutations lead to decreased levels of ATPase by affecting the genes involved in the glucose-signaling pathway (32).

Lower plants and microalgae produce polyunsaturated VLCFAs such as eicosapentaenoic acid and docosahexaenoic acid through the activities of ELOs and desaturases with distinct substrate specificities (33). PSE1 (PUFA specific elongase) cDNA isolated from *Physcomitrella patens*, a moss, has homology with *S. cerevisiae* ELO genes. The enzyme is involved in the elongation of Δ6-PUFAs (polyunsaturated fatty acids) found in *P. patens* and when disrupted production of all C_{20} PUFAs is lost (33).

ELOs have been described in mammals where their functions are being elucidated currenlty. ELO, ELOVL4, impacts the development of Stargardt disease (STGD3) the most common form of inherited macular dystrophy in which the macula (yellow spot near the retina of the eye) atrophies and a degeneration of retinal pigment epithelium is observed (8). Three alleles have been identified for STGD3, each of which results in a truncated ELOVL4 protein that is missing the dilysine ER retention motif; the mislocalization of coexpressed mutant and wildtype ELOVL4 is thought to be the root of at least some of the phenotypic readout (34, 35). Disruption of both copies of ELOVL4 in mice results in a neonatal lethality where missing skin lipids results in the inability to

retain water (36). Another mammalian ELO, ELOVL3 appears to have roles in the synthesis of triacyglycerols in the liver and their accumulation in adipose tissue (37, 38) while the very long chain polyunsaturated fatty acids produced by ELOVL2 are essential for spermatogenesis and male fertility (39). ELOs are classified into two subfamilies based on sequence similarity, which correlates with substrate specificity. ELOs show specificity toward monounsaturated and saturated fatty acids (MUFA/SFA) or toward polyunsaturated fatty acids (PUFA) (40) (Figure 1.5).

Using reconstituted proteoliposomes (41), ELOs have been shown to catalyze the condensation of malonyl-CoA and acyl-CoA, however, little is known about the mechanism through which ELOs catalyze the condensation reaction in the elongation pathway. Alignment of ELOs from different organisms showed highly conserved residues among the ELO family (Figure 1.6); however, there is no conserved Claisen-like condensing enzyme catalytic triad found in ELOs.

Four conserved motifs are found in the ELO family three of which (Figure 1.6, motifs A, C, and D) have no similarity to motifs in other functionally characterized enzyme families. The only conserved motif in ELOs that is familiar is a LHXXHH histidine box (motif B) that is found in enzymes that carry out oxidative reactions (e.g. fatty acid desaturases), where three or four histidine boxes are thought to bind iron (42). The unique characteristics of the ELO sequence suggests that these enzymes carry out the condensation reaction using novel chemistry, an understanding of which may impact the understanding and treatment of diseases.

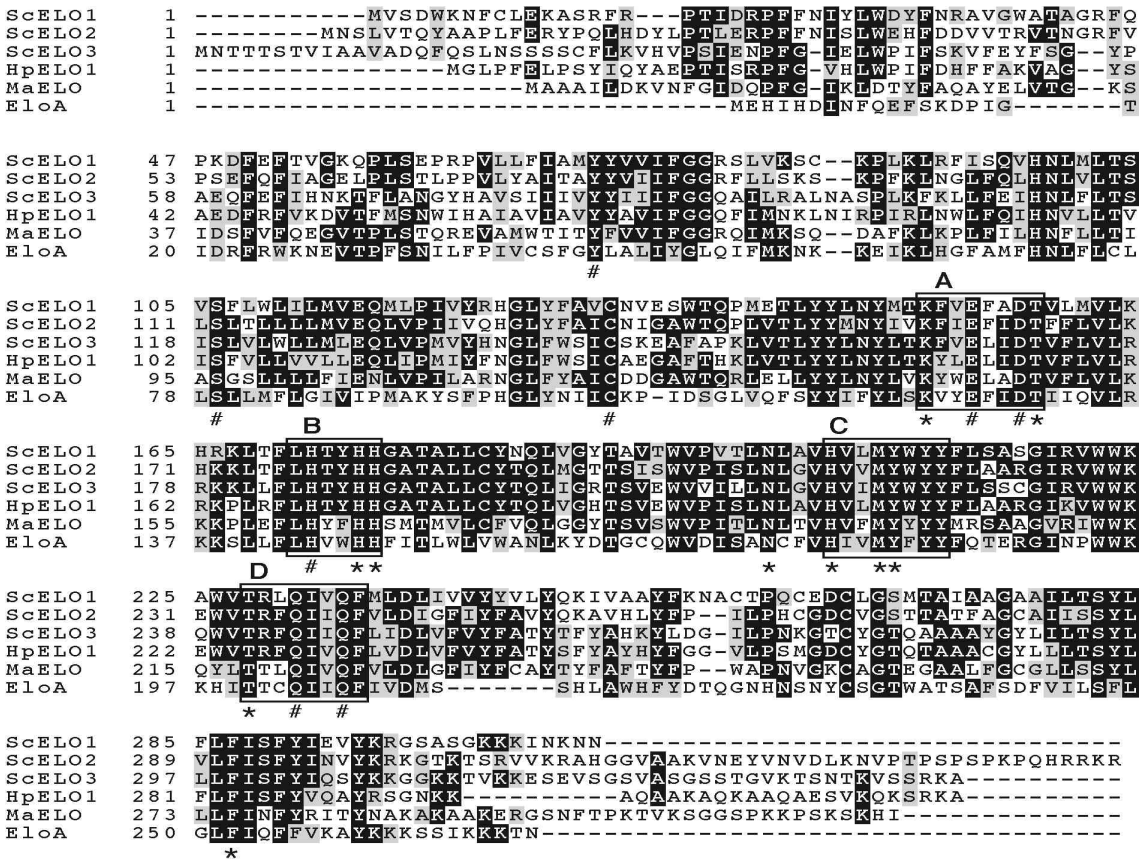

Figure 1.6. Multiple sequence alignment of EloA from *D. discoideum* and related fungal ELOs**.** The four motifs, A, B, C, and D, found in all members of the ELO family are boxed while residues absolutely (*) or highly conserved (#) in all known ELOs are indicated below the EloA sequence. Gene accession #s: *S. cerevisiae* ScELO1, NP_012339; ScELO2, NP_009963; ScELO3, 013476; *Hansenula polymorpa* HaELO1, AB194620; *Mortierella alpina*, AAF71789; and *D. discoideum*, EloA, EU82617.

For this study, an elongase (EloA) model system (17) from the cellular slime mold *Dictyostelium discoideum* (that shows a condensation reaction of $16{:}1^{\Delta 9}$ to $18{:}1^{\Delta 11}$) was used to examine the possible roles of highly conserved residues found in the four conserved motifs among the ELO family in the condensation reaction. A likely low resolution model was generated from the consensus of transmembrane-spanning domain

prediction algorithms (Figure 1.7) (17) to elucidate the orientation of the highly conserved residues along the membrane-spanning domains of EloA. The model predicts that the substrate enters through the cytosol and interacts with those residues present along the four conserved motifs.

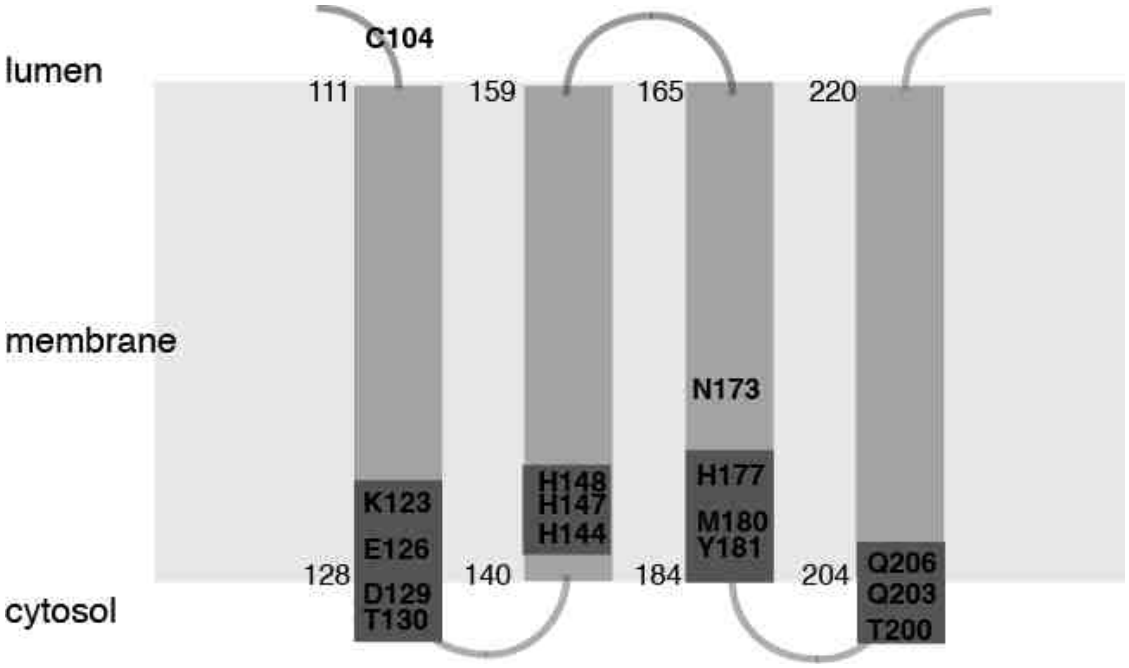

Figure 1.7. Topology model of four key membrane-spanning domains of EloA (17). Dark gray boxes indicate four ELO consensus motifs, within which most of the highly conserved residues in ELOs are found.

1.3 *Dictyostelium discoideum*

Dictyostelium discoideum is a social amoeba that lives in the soil of temperate forests and is used as a model eukaryotic organism. During the amoeboid life stages, *D. discoideum,* ingests bacteria and yeast; however, upon starvation, up to 100,000 cells aggregate and become a multicellular organism. As a result of this transformation, a fruiting body is produced which consists of a stalk that supports a spore head (43, 44) (Figure 1.8). The life stage of *D. discoideum* takes a total of 24 h in a laboratory setting.

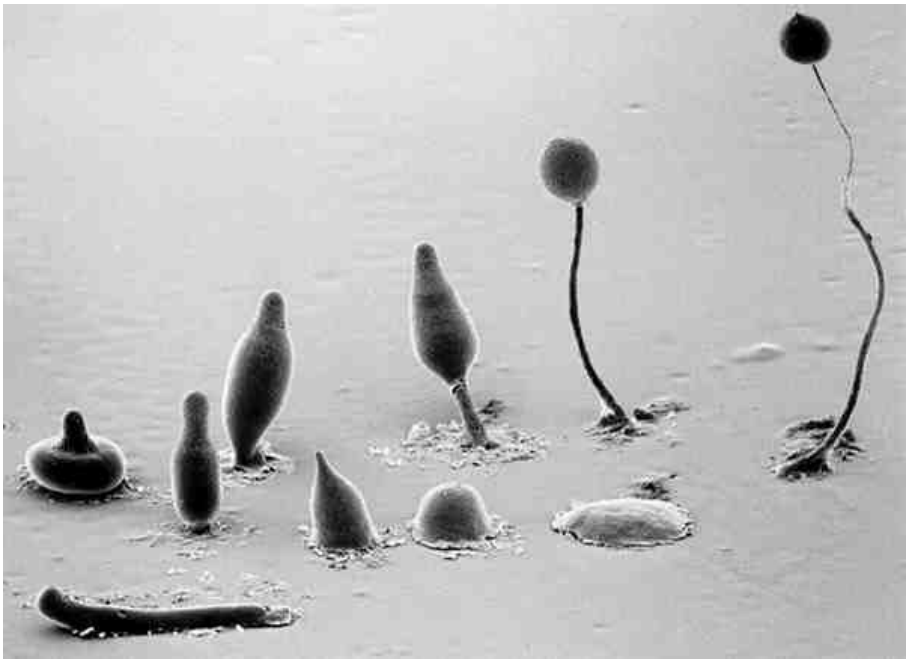

Figure 1.8. Composite electron micrograph of the developmental stages of *D. discoideum* upon starvation. © M.J. Grimson & R. L. Blanton. The micrograph shows the life stages of *D. discoideum*. *D. discoideum* starts as mounds of cells that develop into either a finger-like structure or a migrating slug. After some period of photoaxis, a "Mexican hat" like structure develops which ultimately gives rise to the fruiting body (45).

Phylogenetically, *D. discoideum* is found along the animal branch diverging before fungi; it is more closely related to animals than fungi (Figure 1.9) (43). Important proteins such as those involved in G-protein signaling and cell cycle control (43) found in *D. discoideum* are very closely related to those found in animals thus supporting its closer relationship with animal cells than that observed between yeast and animals (46). The similarity of *Dictyostelium* to animals has prompted is use in the study of human gene orthologues linked to human diseases, e.g., genes linked to cancer, neurological diseases and renal diseases among others (43).

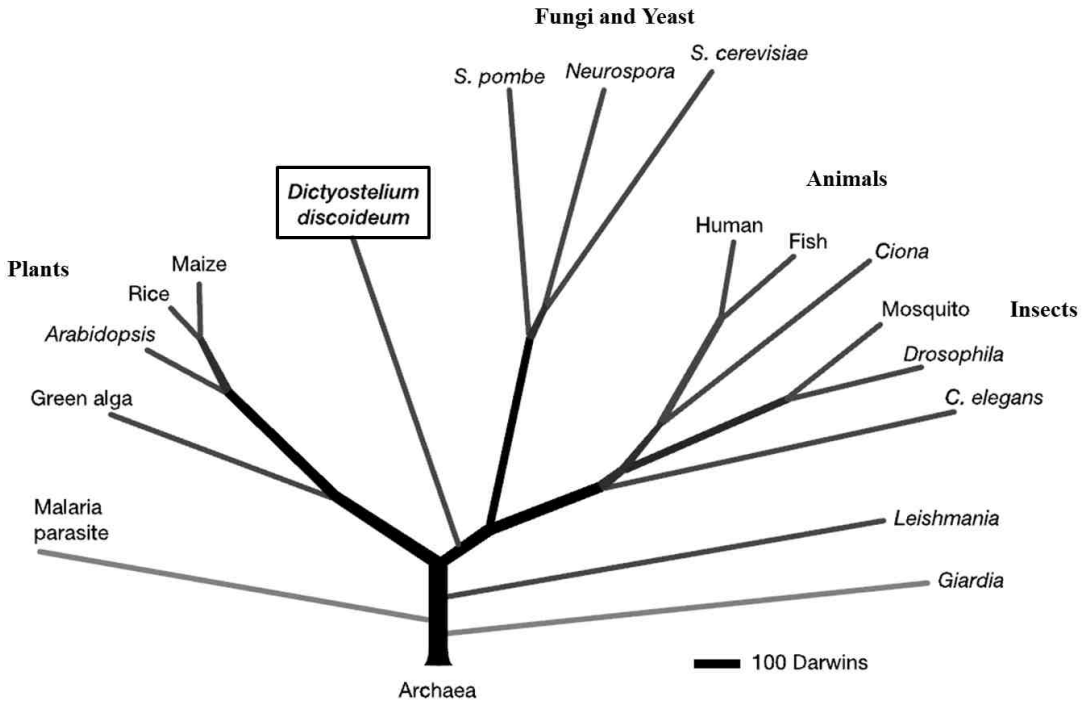

Figure 1.9. Eukaryotic phylogenetic tree illustrating the position of *D. discoideum* (box). The tree was constructed using orthologous protein clusters from eukaryotic proteomes (43).

The unique life cycle of *D. discoideum* makes this organism an excellent candidate to conduct studies examining cell-cell interactions, intracellular/intercellular signaling, cellular differentiation and development, and fatty acid elongation (46). The fatty acid profile of *D. discoideum* shows a variety of fatty acids and VLCFAs with chain lengths ranging from C_{16} to C_{22} and various degrees of unsaturation (Table 1.1) (17). Interestingly, the majority of fatty acids found in *D. discoideum* vegetative cells are Δ^{11}-unsaturated C_{18} fatty acids, suggesting that these fatty acids could be the products of a $16{:}1^{\Delta 9}$ elongation. Further support for a fatty acid elongation pathway in *D. discoideum* is provided by the presence of 20:0 and 22:0 (17).

Table 1.1. Fatty acid profile of *D. discoideum*. Table shows mean percent composition ± sd of fatty acid pyrrolidides prepared from cellular total lipids (17).

Fatty acid	Mean % Composition	Fatty acid	Mean % Composition
16:0	9.42 ± 1.70	18:0	Trace
$16{:}1^{\Delta 5}$	0.97 ± 0.14	$18{:}1^{\Delta 9}$	2.88 ± 0.31
$16{:}1^{\Delta 9}$	6.89 ± 0.44	$18{:}1^{\Delta 11}$	36.56 ± 3.30
$16{:}2^{\Delta 5,9}$	5.14 ± 0.31	$18{:}2^{\Delta 5,11}$	32.27 ± 1.33
17:0	1.38 ± 0.33	$18{:}2^{\Delta 7,11}$	5.90 ± 1.24
$17{:}1^{\Delta 9}$	Trace	20:0	Trace
$17{:}2^{\Delta 5,9}$	1.33 ± 0.09	22:0	2.15 ± 1.07

D. discoideum serves as an important model to study fatty acid elongation as it possess the two types of condensing enzymes, KCSs and ELOs (17) with four ELO genes and one 3-ketoacyl-CoA synthase gene found in this organism. More importantly, research has shown that elongation of unsaturated and saturated fatty acid substrates occurs in *D. discoideum* (17). Previously, a highly active ELO from *D. discoideum* was cloned and characterized in yeast this ELO (EloA) was shown to elongate $16{:}1^{\Delta 9}$ to $18{:}1^{\Delta 11}$ (17).

1.4 Research Objectives

ELOs play an important role in fatty acid elongation and determining their mechanism can lead to a better understanding of this type of enzymes. Additionally, ELOs are known to play important roles in certain diseases and understanding their role may lead to better therapies. Little is known regarding ELOs and how they catalyze condensation reactions. EloA, from *D. discoideum*, possesses characteristic traits found in the ELO family, which makes it a good candidate to conduct biochemical assays that would help us better understand the possible roles of the Histidine box and other motifs conserved in EloA.

In the study outlined herein, site-directed mutagenesis and immunoblotting studies were used to determine if the highly conserved residues found in the ELO family and EloA have a role in ELO structure or function. Table 1.2 shows the targeted amino acids during site-directed mutagenesis. Furthermore, these studies included determining parameters for the solubilization and isolation of this condensing enzyme using hexahistidine fusion proteins as a purified protein is needed to perform specific experiments that will point out exactly what residues, if any, participate in the condensation mechanism.

Table 1.2. Targeted highly and absolutely conserved amino acids in EloA and respective mutations.

Target residue	**Mutation**	**Target residue**	**Mutation**
Tyrosine (Y45)	Alanine	Histidine (H148)	Alanine
Tyrosine (Y45)	Phenylalanine	Asparagine (N173)	Alanine
Serine (S79)	Alanine	Histidine (H177)	Alanine
Cysteine (C104)	Alanine	Methionine (M180)	Alanine
Lysine (K123)	Alanine	Tyrosine (Y181)	Alanine
Glutamic acid (E126)	Alanine	Tyrosine (Y181)	Phenylalanine
Aspartic acid (D129)	Alanine	Threonine (T200)	Alanine
Threonine (T130)	Alanine	Glutamine (Q203)	Alanine
Histidine (H144)	Alanine	Glutamine (Q206)	Alanine
Histidine (H147)	Alanine	Phenylalanine (F252)	Alanine

CHAPTER 2. MATERIALS AND METHODS

2.1 Suppliers

Bacto™ yeast extract, Bacto™ peptone and Fisher Scientific dextrose were used in media preparation. Primers from IDT Integrated Technologies were developed for subcloning and site-directed mutagenesis experiments. The Quick Change II site-directed mutagenesis kit from Stratagene was used to create mutants of EloA. Common molecular biology analysis such as DNA isolation from *E. coli* cells was performed using Promega Wizard Plus Miniprep DNA kit and sequencing reactions for EloA and site-directed mutants were prepared using Applied Biosystems Big Dye Terminator v3.1 Cycle Sequencing kit. Stratagene XL-1 Blue competent *E. coli* cells were used for *E. coli* transformations while Invitrogen InvSc1 *S. cerevisiae* competent cells were used for yeast transformations. Thermo Scientific Triton™ X-100 was used during the solubilization of EloA and tagged fusion proteins.

2.2 *Escherichia coli* Transformation

Stratagene and $RbCl_2$ (47) XL-1 Blue competent *E. coli* cells were used for *E. coli* transformations depending on the experiment. XL1-Blue Stratagene or $RbCl_2$ competent cells (50-100 µl) were incubated with transforming DNA (~10 ng) on ice for 30 min. The mixture was heat-shocked for 45 s in a 42 °C water bath followed by a 2 min incubation on ice. LB media (1 ml, Appendix A) or SOC broth for Stratagene competent cells (500 µl, Appendix A) was added to the mixture and incubated at 37 °C for 1 h with shaking at 250 rpm (New Brunswick, INNOVA 44 Incubator Shaker Series) shaking. Stratagene cells (250 µl) were spread on LB + amp plates (Appendix A) and incubated at 37 °C for 16 h. For $RbCl_2$ transformations, the LB mixture was inverted a couple times followed by an incubation at 37 °C for 1 h. Cells were pelleted at 3,000xg for 30 sec, 900 µl of the supernatant was removed and the remainder was used to resuspend pelleted cells. The cells were spread on LB + amp plates and incubated at 37 °C for 16 h.

2.3 *Saccharomyces cerevisiae* Transformation

S. cerevisiae competent cells (InvSc1, Invitrogen) were prepared by growing cells in 100 ml YPAD (Appendix A) rich media at 30 °C with shaking at 250 rpm until an optical density at 600 nm (OD_{600}) of 0.5-0.7 A was reached. The grown cells were pelleted for 5 min at 1,900xg (IEC HN-SII Centrifuge, Damon) and resuspended in 0.1 M LiAc, 10 mM Tris, 1mM EDTA pH 8.0 to an OD_{600} of 0.6 A. Competent cells were stored on ice at 4 °C over night. Transformations were carried out by the lithium acetate method (48) which required 100 µl of pelleted competent cells followed by layered 240

µl 50% PEG 3350, 36 µl 1 M LiAc, 25 µl 2 mg/ml salmon sperm DNA, sample DNA (100-200 ng/ µl) and water. Cells were gently resuspended by pipetting and incubated at 30 °C for 30 min followed by a 25 min incubation at 42 °C. The mixture was centrifuged for 2 min at 3,000xg, the supernatant was removed and cells were resuspended with 250 µl of water. Transformants were selected for growth on complete minimal media plus 2% dextrose plates (cm-his/ura + 2% dextrose, Appendix A), depending on the transforming plasmid, for three days at 30 °C.

2.4 Site-Directed Mutagenesis of Conserved Residues in EloA

Highly conserved residues in the ELO family, determined by Clustal W2 (DNA Star) (17) multiple sequence alignment of ELOs from different organisms (Figure 1.6), were mutated using the Quik Change II Site-Directed Mutagenesis Kit (Stratagene, La Jolla, CA). Forward and reverse primers (Integrated DNA Technologies, Coralville, IA) were designed to mutate the targeted residue to either alanine (GCT, GCC, GCA) or phenylalanine (TTT) (Table 2.1) and prepared at a stock concentration of 2000 ng/µl. The mutagenesis extension reactions were prepared as described by the manufacturer (Table 2.2) with EloA inserted into the vector pESc-His (Statagene) as the template.

Table 2.1. Site-directed mutagenesis forward (F) and reverse oligonucleotide primers (not shown, complementary to forward primers) were used to introduce alanine or phenylalanine mutations into the EloA gene using the QuikChange II Site-Directed Mutagenesis Kit. Letters in bold indicate those nucleotides that were different from the wild-type sequence.

Mutation	Primer Sequence
Y45A	F: 5'-GTATGTTCATTTGGT**GC**TTTGGCATTAATTTAT
Y45F	F: 5'-GTATGTTCATTTGGT**T**TTTTGGCATTAATTTAT
S79A	F: 5'-AATTTATTCTTATGTTTATTA**GC**ATTATTAATGTTTTTAGGTATT
C104A	F: 5'-CATGGTTTATACAATATAATT**GC**TAAACCAATTGATAGTGGTTTA
K123A	F: 5'-CAGTTATTACATTTTCTATCTTAGT**GC**AGTTTATGAATTTATTGATACAATAATTCAAG
E126A	F: 5'-TTCTATCTTAGTAAAGTTTATG**CA**TTTATTGATACAATAATTCAA
D129A	F: 5'-CTTAGTAAAGTTTATGAATTTATT**GC**ACAATAATTCAAGTTTTA
T130A	F: 5'-ATGAATTTATTGAT**GC**AATAATTCAAGTTTTA
H144A	F: 5'-AAGTTTATTATTTTTA**GC**TGTATGGCATCAT
H147A	F: 5'-ATTTTTACATGTATGG**GC**TCATTTCATTACATT
H148A	F: 5'-TACATGTATGGCAT**GC**TTTCATTACATTATG
N173A	F: 5'-GTCAATGGGTAGATATTTCAGCA**GCT**TGTTTCGTTCATATTGTTATGTAC
H177A	F: 5'-GATATTTCAGCAAATTGTTTCGTT**GC**TATTGTTATGTACTTTTATTATTTCCAAAC
M180A	F: 5'-CGTTCATATTGTT**GCC**TACTTTTATTATTTCC
Y181A	F: 5'-CAGCAAATTGTTTCGTTCATATTGTTATG**GC**CTTTTATTATTTCCAAACGTAACGTGG
Y181F	F: 5'-GTTTCGTTCATATTGTTATG**TT**CTTTTATTATTTCCAAACTGAAC
T200A	F: 5'-GGAAAAAACATATT**GC**AACTTGTCAAATCATACAATTCATAGTTG
Q203A	F: 5'-ATTACAACTTGT**GC**AATCATACAATTCATAGTTGATATGAGTTCAC
Q206A	F: 5'-CTTGTCAAATCATA**GC**ATTCATAGTTGATATG
F252A	F: 5'-ATTTTATCATTCCTTGGTTTA**GC**CATTCAATTCTTTGTAAAAGCA

Table 2.2. Site-directed mutagenesis reactions, as specified by manufacturer.

Ingredient	Amount
10X Reaction buffer: 100 mM KCl, 100 mM $(NH4)_2SO_4$, 200 mM Tris-HCl, 200 mM $MgSO_4$, 1% Triton X-100, 1 mg/ml BSA	2.5 µl
template	25 ng
forward oligonucleotide primer	62.5 ng
reverse oligonucleotide primer	62.5 ng
dNTP mix	0.5 µl
molecular biology H_20	up to 25 µl
Pfu Ultra High-Fidelity DNA polymerase (25 U/µl)	0.5 µl

The mutagenesis primers were extended during temperature cycling (Eppendorf Gradient Cycler) as indicated in Table 2.3. Following the generation of the mutated plasmid, the parental DNA was digested with 0.5 µl *Dpn* I restriction enzyme (10 U/µl) for 1 h at 37 °C. After *Dpn* I digestion of the parental template, the mutated plasmids were transformed into *E. coli* XL-1 Blue (Stratagene) cells and grown on LB + amp for 16 h at 37 °C. Transformants were picked and grown in LB + amp (5 ml LB with 0.1 mg/ml ampicillin) for 16 h with shaking (250 rpm) at 37 °C. The plasmids were isolated and purified by Wizard Plus Miniprep DNA kit (Promega, Madison, WI) and sequenced with BigDye® Terminator v3.1 Cycle Sequencing Kit (Applied Biosystems Foster City, CA) using vector-directed primers (Gal 1) to confirm the installation of the desired mutation (Table 2.4, Table 2.5).

Table 2.3. Site-directed mutagenesis temperature cycling parameters

Step	Temperature	Time
1	95 °C	30 s
2	95 °C	30 s
3	55 °C	1 min
4	68 °C	6 min
Go to 2, repeat 24 times, hold at 4 °C		

Table 2.4. Cycle sequencing reactions

Ingredient	Amount
template	300 ng
primer (Forward/Reverse)	2 µM
5x BigDye sequencing buffer	3 µl
terminator ready reaction mix	2 µl
molecular biology H_2O	up to 20 µl

Table 2.5. BigDye Terminator cycle sequencing parameters

Step	Temperature	Time
1	96 °C	1 min
2	96 °C	10 sec
3	50 °C	5 sec
4	60 °C	4 min
Go to 2, repeat 24; hold at 4 °C		

Extension products were purified by ethanol/EDTA/sodium acetate precipitation with 3 M sodium acetate/0.5 M sodium ethylenediaminetetraacedic acid, pH 8.0 (2 µL) and 80 µL 95% ethanol and centrifuged for 15 min at 16,100xg (Eppendorf Centrifuge 5415R). The pellet was treated with 125 µl of cold 70% ethanol followed by centrifugation for 15 min at 16,100xg centrifugation to remove salt residue and samples were allowed to air dry.

The samples were sent to Miami University Center for Bioinformatics and Functional Genomics for sequencing and the resulting sequences and electropherograms were analyzed using Lasergene® SeqMan Pro (DNASTAR, Madison, WI) where the forward and reverse sequences were aligned with the wild-type sequence to confirm the presence of the desired mutation

2.5 Fatty Acid Methyl Ester Preparation and Analysis

Single *S. cerevisiae* transformed colonies were grown in 5 ml YPAD rich media for 16 h at 30˚C with shaking at 250 rpm. Expression cultures (5 ml, cm-his + 2% galactose) were inoculated with 50 µl of starter culture and grown at 30˚C with shaking at 250 rpm for 3 days. Equal cell numbers were collected by centrifugation for 5 min at 1,900xg and the supernatant removed. Fatty acid methyl esters (FAMEs) were prepared by transesterification with 2% sulfuric acid in methanol (0.5 ml) and incubation at 80˚C for one hour.

Prepared FAMEs were extracted from the transesterification reactions upon addition of 0.5 ml H_2O with hexanes (2 x 1 ml) and dried under N_2 gas. Hexanes (200 µl) were added to redissolve the FAME sample which was analyzed by gas chromatography/mass spectrometry (GC/MS) with an Agilent Technologies 7890A GC/5975C MS and HP5 column (J & W Scientific) using the following oven conditions: 100 °C for 3 min, ramp 30 °C/min to 200 °C, ramp 2.5 °in to 250 °C, ramp10 °C/min to 290 °C and hold for 1 min, decrease 60 °C/min to 100 °C.

2.6 Microsome Preparation from Yeast Expressing EloA

To make microsomes from EloA-expressing yeast, YPAD starter cultures (5 ml) were inoculated with a single transformant and grown for 16 h at 30°C with shaking (250 rpm). Expression cultures (40 ml, cm-his + 2% galactose) inoculated with 0.4 ml of starter culture were grown overnight at 30˚C with shaking (250 rpm) (14). Cells were pelleted by centrifugation at 1,900xg for 5 min, resuspended in isolation buffer (IB; 80 mM Hepes-KOH pH 7.2, 10 mM KCl, 320 mM sucrose, 5 mM EDTA pH 8.0, 5 mM EGTA pH 8.0, 0.1 M PMSF and 31 µg/mL benzamidine) and lysed by homogenization (three times for 1 min with 2 min ice incubations between each bead beating) with glass beads (0.5 mm beads) on a Bead Beater (BioSpec Products).

Unlyzed cells and debris were removed by quick microcentrifugation (12 sec x2; max speed 13,000xg) and collecting only the supernatant. Microsomes were collected from the lysate diluted to 40 ml with IB by ultracentrifugation for 1 h at 50,000xg at a temperature of 4°C and the pellets resuspended in IB (200 µl). The protein concentration of each sample was determined by the Bradford method (49) (Sigma-Aldrich, St. Louis, MO) using BSA as a standard and adjusted to 2.5 µg/µl by addition of IB and glycerol to 15% (v/v). Samples were frozen on dry ice and stored at -80 °C.

2.7 EloA Expression Analysis by Immunoblot

Polyclonal antibodies (Cocalico Biologicals Inc, Reamstown, PA) were raised against a synthesized peptide derived from the EloA amino terminus (residues 1-20) and used in immunoblot assays to determine protein expression levels. Microsomal protein (20 μg) treated with Laemmli buffer (50) was denatured for 5 min at 95 °C and separated on a 12% SDS-PAGE gel (Appendix A) at 100 V through stacking gel and then 140 V through the resolving gel. The separated proteins were transferred to a methanol-rinsed, transfer buffer pre-incubated in transfer buffer (30 min, Appendix A) Immobilon-P (Millipore) polyvinylidene fluoride membrane in transfer buffer with an ice pack and stirred for 2 h at 100 V (BioRad Mini Trans-Blot Cell, Hercules, CA).

After transfer, the membrane was blocked with TTBS (100 mM Tris, pH 7.5, 150 mM NaCl, 0.1% Tween 20) over night at 4°C and then incubated with anti-EloA (1/500 dilution in TTBS) mixed with anti-Erg27p (1/300 dilution in TTBS; gift from Martin Bard, IUPUI) for 2 h with gentle shaking at room temperature. The levels of EloA and Erg27p were detected upon incubation with goat-anti rabbit IgG horseradish peroxidase conjugate (Biorad; 1/2500 dilution in TTBS) for 1.5 h with gently shaking at room temperature followed by chemiluminescent detection (Pierce SuperSignal West Pico) on a photodocumentation system (BioRad Quantity One® 1-D Analysis Software; 2 min exposure at 15 second increments).

2.8 Engineering of N- and C-Terminally His_6-tagged EloA Expression Plasmids

Two different fusion proteins, one tagged at the amino (His_6-EloA) terminus (Figure 2.1) and another tagged at the carboxy (EloA-His_6) terminus, were constructed for the characterization of EloA. The His_6-EloA plasmid was constructed from an available pYES2 vector (Invitrogen) designed for fusion of the hexahistidine tag at the amino terminus. EloA was amplified using primers containing restriction sites EcoRI at the 3' and BamHI at the 5', convenient for subcloning into pYES2 tagged yeast expression vector. The EloA-His_6 plasmid was designed by creating primers (Table 2.6) that incorporated a hexahistidine tag at the carboxy terminus of EloA and included a BamHI site (5') after the tag to allow in-frame subcloning into the pYES2 vector.

Table 2.6. Amplification primers used during subcloning of EloA into pYES2

Primers	Sequence
Reverse EcoRI His_6-EloA	5'-GGGGAATTCTTAATTTGTTTTCTTTTTAATTGAAG-3'
Forward BamHI His_6-EloA	5'-GGG GGA TCC ATG GAA CAT ATT CAT GA-3'
Reverse EcoRI EloA-His_6	5'- ATC TTC ATT AAA AAG AAA ACA AAT $(CAT)_6$ TAA-3'

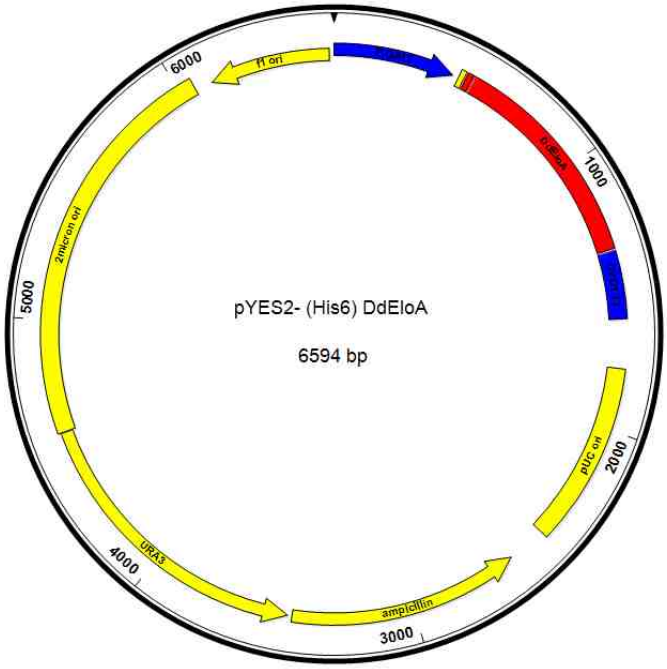

Figure 2.1. The His_6-EloA plasmid map (6594 bp) illustrates EloA subcloned into the yeast expression vector pYES2. The map shows the presence of the hexahistidine tag (blue block) and the Gal1 promoter (blue arrow).

The gene amplification reactions contained 2 µl of 10x amplification buffer (100 mM Tris-HCl pH 8.3, 500 mM KCl and 20 mM $MgCl_2$), 2 µl of each 2 mM dNTP stock, 0.2 µl Vent polymerase, 2 µl of template, 2 µl of each respective primer (5 µM stock) and 3.8 µl of water and were amplified as outlined in Table 7. PCR products were purified using QIAquick PCR purification kit protocol by QIAgen (Valencia, CA).

Table 2.7. EloA Polymerase Chain Reaction Amplification parameters

Step	Temperature	Time
1	94 °C	2 min
2	94 °C	15 s
3	65 °C	15 s; increment step temp by -1 °C
	R=3 °/s	+0.0°/s
	G= 0.0 °	
4	72 °C	1 min
5	go to 2, repeat 15	
6	94 °C	15 s
7	50 °C	15 s
8	72 °C	1 min
9	go to 6, repeat 20	
10	72 °C	2 min
11	hold at 4 °C	

The purified PCR products were digested with BamHI and EcoRI (Table 2.8) and incubated at 37 °C for 1 h. Digested products were purified by QIAEX II Gel extraction kit protocol by QIAgen (Valencia, CA) and ligated into the vector with T4 DNA ligase (Life Technologies, Gibco-BRL). The ligation reactions contained 4 µl 5x ligase buffer, 2 µl 10 mM ATP, 1 µl ligase, 6:1 insert to vector (v/v), and molecular biology water up to 20 µl. Reactions were incubated overnight at room temperature. The ligation reactions (10 µl) were transformed into $RbCl_2$ competent *E. coli* as described previously. Insert-containing plasmids were isolated by Wizard Plus Miniprep DNA kit and sequenced to rule out mutations.

Table 2.8. Set up for digestion reactions.

Vector: His_6pYES2		Insert: EloA	
Ingredient	Amount	Ingredient	Amount
vector DNA	3.8 µl (0.34 µg/ µl)	insert DNA	20 µl (0.07 µg/ µl)
10X NEB 3 Buffer	5 µl	10X NEB 3 Buffer	5 µl
100X BSA	0.5 µl	100X BSA	0.5 µl
Bam HI	1 µl	Bam HI	1 µl
EcoRI	1 µl	EcoRI	1 µl
Molecular Biology H_2O	up to 20 µl	Molecular Biology H_2O	up to 20 µl

The yeast expression vector encoding the carboxy terminally-tagged EloA was constructed in a similar matter as that described for the amino tagged EloA and using a developed primer containing the hexahistidine tag (Table 2.6). Plasmids were transformed into competent *S. cerevisiae* (InvScI, Invitrogen) as previously described.

2.9 Solubilization and Isolation of His_6-EloA

Microsomes prepared from yeast expressing His_6-tagged EloA fusion protein and those transformed with vector pYES2 were solubilized by incubation on ice for 2 h in solubilization buffer (320 mM NaCl, Triton X-100, in IB; 2 µg protein/µl). Different percentages of Triton X-100 (0.1, 0.05, and 0 % v/v) were used during the solubilization experiments. Insoluble material was pelleted by centrifugation at 4°C for 1 h at 16,100xg. Supernatants were frozen on dry ice and stored at -80°C.

Supernatants were combined with binding buffer (25 mM sodium phosphate, pH 8.0, 0.5% Triton X-100, 150 mM NaCl and 10% glycerol (v/v)) at a ratio 0.43:1 (supernantant:binding buffer) and applied to a 300-µl column of Ni-NTA Agarose resin (QIAgen) or TALON Cobalt affinity resin (Clontech, Palo Alto, CA). The Ni/Co column was washed with 1 ml binding buffer, 1 ml wash buffer (25 mM sodium phosphate, pH 8.0, 0.5% Triton X-100, 500 mM NaCl, 10% glycerol, and 20 mM imidazole), and 1 ml binding buffer. Protein elution from the column was performed with 300 µl elution buffer (25 mM sodium phosphate, pH 8.0, 0.5% Triton X-100, 500 mM NaCl, 10% glycerol, and 300 mM imidazole) and dithiothreitol was added to 2 mM to the eluted fraction. Eluted protein samples were frozen on dry ice and stored at -80°C.

2.10 Condensation Assay

Condensation activity was assayed as described previously (15, 27). Material eluted from Ni/Co column (5 µl) was incubated with condensation reaction mix (20 µl; 10 mM sodium phosphate, pH 7.2, 0.05% Triton X-100, 15 µM [2-^{14}C] malonyl-CoA and 20 µM 16:1-CoA, H_2O) at 30°C for 1 h. The reaction products were reduced to diols by incubation with 0.5 ml of reducing agent (0.132 M $NaBH_4$, 0.143 M K_2HPO_4, 0.57 M KCL and 30% distilled tetrahydrofuran) at 37°C for 30 min followed by the addition of 15 µl of 12 N HCl. The products were extracted into pentane (2 x 0.8 mL), evaporated under a N_2 stream and quantified by methylene chloride liquid scintillation (Fisher Scientific) analysis using a Beckman LS 6000 Liquid Scintillation Counter. As a negative control, empty vector mock-isolated samples were assayed in a similar matter.

CHAPTER 3. RESULTS

3.1. Introduction

Sequence alignment of functionally characterized ELOs identified a number of highly conserved residues and four ELO family consensus motifs (17). The main objective of the research described here was to analyze the possible role(s) of these residues found within the ELO family. Although we do not know how ELOs catalyze the condensation reaction due to their lack of homology to other characterized condensation enzymes, we hypothesized that highly conserved residues found in ELOs from different organisms have a pivotal catalytic and/or structural function for the enzyme. A model elongase condensing enzyme (EloA) (17) from the cellular slime mold, *D. discoideum*, shows a substrate specificity for monounsaturated fatty acids catalyzing the condensation reaction for the elongation of $16{:}1^{\Delta 9}$ to $18{:}1^{\Delta 11}$ and was used to examine the possible roles of these residues in the condensation reaction. In addition, preliminary work was carried out to establish experimental parameters for the isolation of the *D. discoideum* condensing enzyme, EloA, upon heterologous expression in yeast to aid in the future characterization of this membrane-bound protein.

Site-directed mutagenesis was used to target absolutely and highly conserved residues found in the ELO family. The targeted residues were replaced with alanine or, in the case of tyrosine residues, to alanine or phenylalanine.

For this study, twenty mutants were made and expressed in yeast; FAMEs prepared from total yeast lipids were analyzed by GC/MS to determine the level of EloA activity. Semi-quantitation of expressed mutant and wild-type EloA protein levels were performed to examine the importance of these condensing enzymes during fatty acid elongation.

3.2. Activity of EloA Site-Directed Mutants FAMEs Analysis

The activities of wild-type and mutant EloA enzymes were examined upon expression in *S. cerevisiae* through the preparation of FAMEs from total yeast lipids followed by GC/MS analysis. The separation of yeast-derived FAMEs, produced in the absence (A) and presence of EloA (B) was demonstrated by total ion chromatographs (TIC; Figure 3.1). Fatty acid methyl esters observed in the TICs included $16{:}1^{\Delta 9}$ (10.5 min), 16:0 (10.7 min), $18{:}1^{\Delta 9}$ (13.3 min), $18{:}1^{\Delta 11}$ (13.4 min), 18:0 (13.8 min) and 20:1 (17.9 min, B). The yeast empty vector (EV, A) used for expression of EloA and site-directed mutants has endogenous elongases that show background elongation activity thus providing a small percentage of the $18{:}1^{\Delta 11}$ elongation product. In order to account for this background activity, empty vector samples were prepared and analyzed in the same manner as were the mutant samples. Compared to yeast transformed with EV, yeast expressing EloA had a higher percentage of elongation product $18{:}1^{\Delta 11}$ and the production of a new fatty acid 20:1.

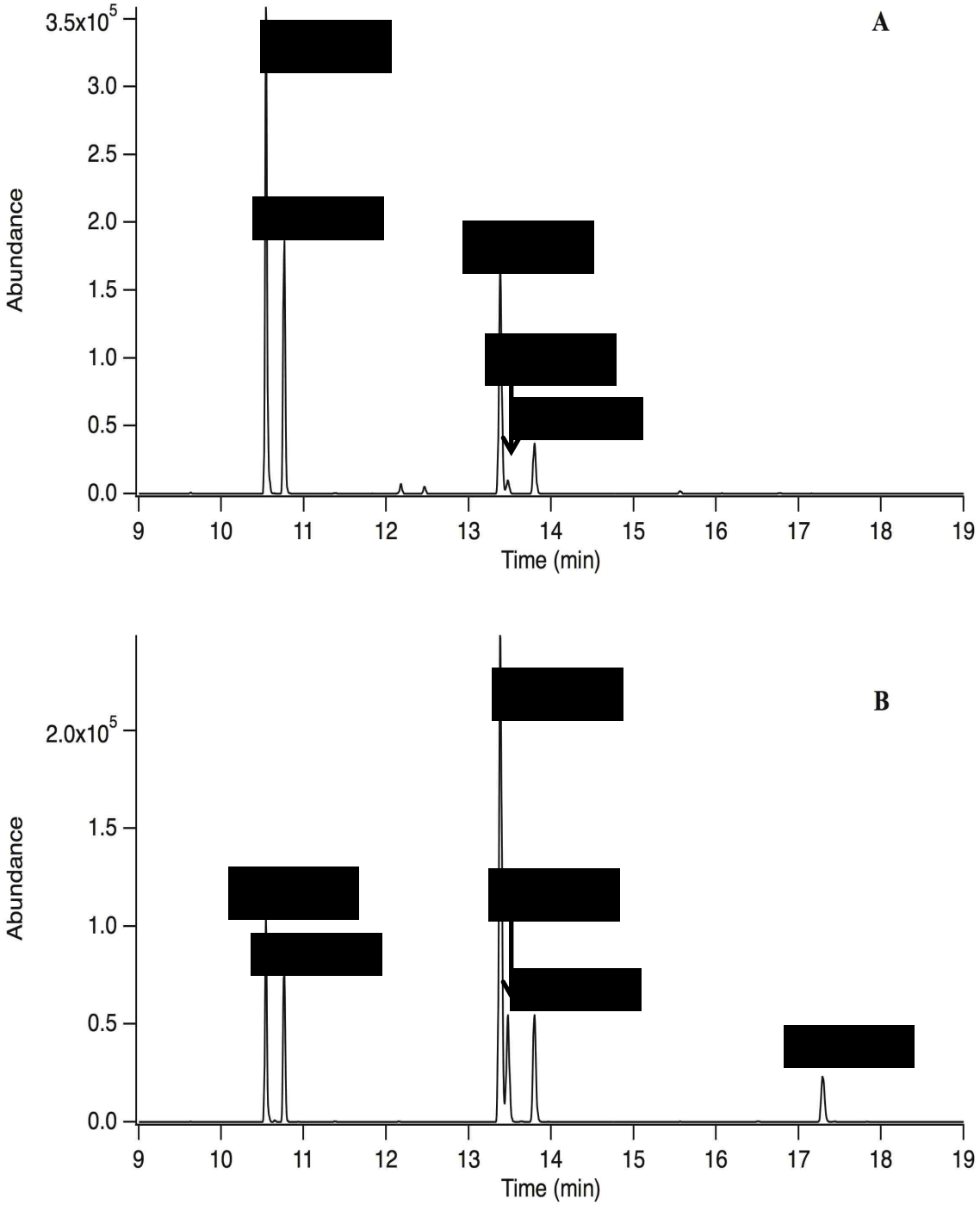

Figure 3.1. Total Ion Chromatogram (TIC) of FAMEs from yeast expressing empty vector (EV) pESc (A) and EloA (B).

FAME analysis showed that yeast transformed with empty vector or wild-type EloA had different fatty acids profiles (Table 3.1). One of the major differences between the empty vector and wild-type EloA was the decrease in 16:1 $^{\Delta 9}$ and a reciprocal increase in 18:1$^{\Delta 11}$. The yeast transformed with empty vector showed a mean of 39.4 ± 3.3% for 16:1$^{\Delta 9}$ versus a mean of 17.5 ± 1.4% seen in yeast expressing wild-type EloA. However, the percentage of 18:1$^{\Delta 11}$ observed in yeast that expressed empty vector was a mean of 1.8 ± 0.3% versus a mean of 10.9 ± 0.5% seen in yeast expressing wild-type EloA. The increase in the amount of the 18:1 $^{\Delta 11}$ elongation product demonstrates the elongase activity of EloA.

The fatty acid profile of yeast expressing each of the EloA site-directed mutants is presented in Table 3.1 and Figure 3.2. Upon analysis of the percentage of the EloA elongation product, site-directed mutants were grouped into three groups based on their activity relative to the wild-type enzyme: those within 20% of wild-type activity (10.1-11.5% 18:1$^{\Delta 11}$) (Y45F, S79A, H144A, and Y181F); those with between 10 and 60% of wild-type activity (4.0-8.0% 18:1$^{\Delta 11}$; Y45A, C104A, E126A, M180A, Y181A, T200A); and those with little or no activity (1.9-3.5% 18:1$^{\Delta 11}$; K123A, D129A, T130A, H147A, H148A, N173A, H177A, Q203A, Q206A, and F252A) (Figure 3.2). The mutants with little or no activity had similar percentages of the other fatty acids (16:0, 16:1$^{\Delta 9}$, 18:0) as those observed in the empty vector (Table 3.1). The mutants within 20% and those within 10 and 60% of wild-type activity showed relatively similar percentages of other fatty acids as those observed in EloA.

Table 3.1. Fatty acid profiles of *S. cerevisiae* expressing EloA and site-directed mutants. The % fatty acid of total fatty acids, determined by FAMEs analysis produced from total yeast cells, are expressed as the mean ± sd, n = 5-6.

% FA ± sd	16:0	$16:1^{\Delta 9}$	18:0	$18:1^{\Delta 9}$	$18:1^{\Delta 11}$
EV	23.7 ± 1.1	39.4 ± 3.3	7.4 ± 1.4	27.7 ± 0.7	1.8 ± 0.3
EloA	11.6 ± 0.2	17.5 ± 1.4	11.8 ± 1.3	48.2 ±1.2	10.9 ± 0.5
Y45A	17.6 ± 1.6	27.9 ± 2.1	11.3 ± 1.8	37.1 ± 1.0	6.0 ± 0.4
Y45F	13.7 ± 0.4	19.5 ± 1.2	16.0 ± 1.2	39.3 ± 0.9	11.5 ± 1.2
S79A	13.6 ± 0.7	20.1 ± 2.8	15.3 ± 1.7	40.6 ± 1.9	10.4 ± 0.5
C104A	17.4 ± 0.3	28.8 ± 0.6	13.5 ± 0.4	32.3 ± 0.5	8.0 ± 0.3
K123A	21.3 ± 1.7	34.1 ± 8.2	10.1 ± 2.3	32.4 ± 5.2	2.2 ± 0.4
E126A	17.0 ± 0.3	30.2 ± 1.4	9.7 ± 1.3	37.0 ± 0.8	6.2 ± 0.3
D129A	20.5 ± 1.0	35.5 ± 6.2	9.1 ± 1.4	32.6 ± 4.3	2.2 ± 0.6
T130A	20.7 ± 0.9	30.9 ± 2.9	9.2 ± 1.6	35.9 ± 5.4	3.4 ± 0.9
H144A	12.2 ± 0.7	20.1 ± 2.6	12.0 ± 3.1	45.6 ± 0.8	10.2 ± 0.5
H147A	23.3 ± 0.7	39.9 ± 2.8	8.7 ± 0.8	25.3 ± 2.1	2.3 ± 0.2
H148A	20.6 ± 1.2	36.4 ± 3.0	8.3 ± 0.7	32.1 ± 1.4	2.6 ± 0.3
N173A	22.3 ± 1.4	34.6 ± 4.8	9.4 ± 1.5	31.4 ± 4.0	2.2 ± 0.4
H177A	22.9 ± 1.0	37.5 ± 2.9	7.6 ± 1.0	30.1 ± 1.2	1.9 ± 0.2
M180A	15.9 ± 0.6	26.7 ± 1.8	11.2 ± 2.6	39.1 ± 1.2	7.1 ± 0.6
Y181A	18.2 ± 1.2	30.7 ± 5.5	12.3 ± 2.9	34.6 ± 3.0	4.3 ± 0.9
Y181F	12.8 ± 0.5	18.0 ± 2.8	11.8 ± 1.1	47.3 ± 1.3	10.1 ± 0.7
T200A	19.6 ± 2.7	28.8 ± 2.6	12.0 ± 1.3	35.6 ± 1.9	4.0 ± 0.7
Q203A	21.5 ± 1.2	35.5 ± 2.1	8.6 ± 0.9	31.7 ± 1.5	2.7 ± 0.4
Q206A	21.5 ± 0.2	34.8 ± 0.5	10.8 ± 0.2	29.5 ± 0.2	3.5 ± 0.1
F252A	21.5 ± 0.6	32.7 ± 0.8	12.1 ± 0.4	30.2 ± 1.1	3.4 ± 0.2

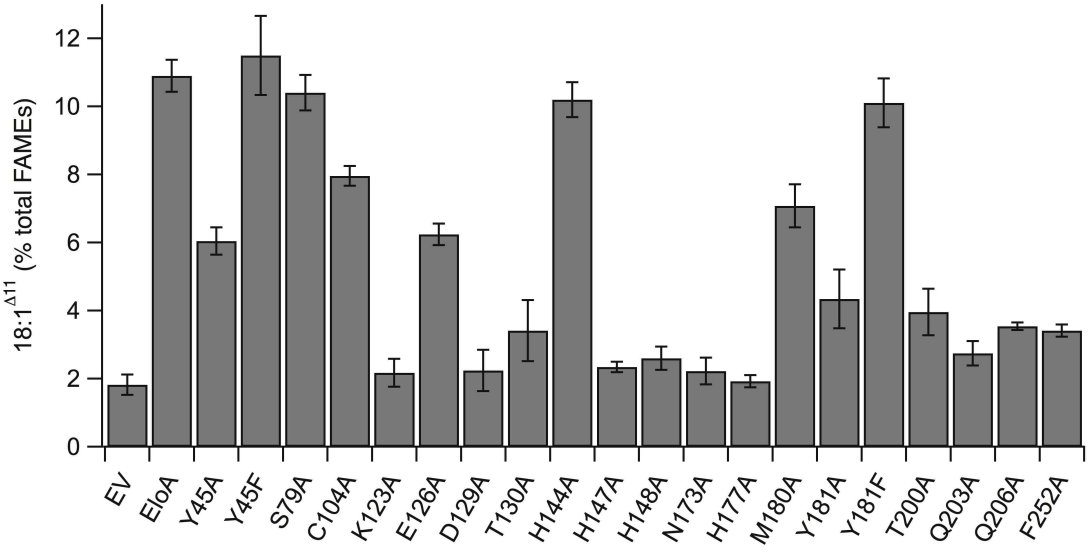

Figure 3.2. Production of $18:1^{\Delta 11}$ by EloA site-directed mutants. Fatty acid methyl esters prepared from total yeast cellular lipids were analyzed by GC/MS. $18:1^{\Delta 11}$ as a percent of total FAMEs is presented as the mean +/- sd; n=5 or 6. Note that *S. cerevisiae* has a low level of endogenous activity producing close to 2% of the total FAMEs.

The activity of mutants within 20% of wild-type activity demonstrated that mutations of the conserved residues (Y45F, S79A, H144A, and Y181F) did not disrupt the function of the enzyme and that it is still able to produce wild-type like percentages of $18:1^{\Delta 11}$. In contrast, the mutants with little to no activity of wild-type (K123A, D129A, T130A, H147A, H148A, N173A, H177A, Q203A, Q206A, and F252A) suggested that the amino acid residue changes at these positions disrupt the production of the main EloA product, $18:1^{\Delta 11}$.

Based on the levels of activity of the EloA mutants, a number of the residues explored appear to be involved in maintaining the correct structure of the protein. The tyrosine residues (Y45 and Y181) were mutated to both alanine and phenylalanine and the activity of the tyrosine to phenylalanine mutants for both residues was within 20% of

the wild-type activity. In contrast, when the tyrosine residues were mutated to alanine, a drastic decrease in activity was observed (46% and 28% of wild-type activity, respectively). The disturbance in activity levels for the alanine mutant strongly suggests the participation of the tyrosine residue as a structural factor.

3.3. EloA Expression Analysis by Immunoblot

The analysis of FAMEs prepared from yeast expressing the wild-type and mutant EloA only reflects the activity of the enzyme *in vivo*; therefore, site-directed mutants were analyzed by immunoblot assay to determine EloA expression levels. Microsomes prepared from yeast expressing wild-type EloA and each mutant allele as well as yeast transformed with the empty expression vector were simultaneously probed with anti-EloA and anti-Erg27p sera. Erg27p is a 3-keto-reductase microsomal protein that participates in the C-4 demethylation of ergosterol biosynthesis intermediates in yeast (51) and was used as a loading control for total microsomal protein (Figure 3.3).

Figure 3.3. Immunoblot analysis of microsomes prepared from yeast expressing wild-type and mutant EloAs. Microsomal protein (20 μg) was analyzed by immunoblot with anti-EloA and anti-Erg27.

As expected, lanes loaded with microsomes derived from yeast transformed with the empty vector (pESc, EV) showed only a band corresponding to the loading control Erg27p (molecular mass = 39.7 kDa), while the lanes loaded with microsomes prepared from yeast expressing wild-type EloA and each mutant had two bands: the loading control and EloA (molecular mass = 32.2 kDa). The immunoblot assay results indicated that the absence of EloA activity in yeast expressing the K123A, D129A, H147A, H177A, Q203A, Q206A, and F252A mutants demonstrated at least an equivalent level of staining with anti-EloA and a comparable ratio between EloA and LC staining as the wild-type.

Furthermore, most of the mutants showed at least comparable staining with anti-EloA as the wild-type. This suggests that the decreases in activity exhibited by these site-directed mutants is not a result of protein expression levels but the effects of the residue mutation on the activity of the enzyme. This observation again highlights the importance of the highly conserved residues. An exception is M180A, which has a higher level of EloA protein staining compared to the wild-type enzyme. M180A is a member of the group of mutants with 10 and 60% wild-type activity and the staining seen for the LC is comparable to the EV suggesting that this mutant allele expressed more EloA.

3.4. Study of His_6-tagged EloA Expression through Analysis of FAMEs and Immunoblot

After *in vivo* analysis of the wild-type and site-directed mutants, the optimal conditions to solubilize and perform preliminary isolation experiments of EloA were determined. Determining optimal conditions for the solubilization and isolation of EloA would aid in the future characterization of this membrane-bound ELO. The first step was to tag wild-type EloA by adding a hexahistidine tag at the amino and carboxy termini, separately. The tagged protein was then utilized to determine preliminary parameters and conditions for the solubilization and subsequent isolation of EloA.

Expression plasmids for EloA hexahistidine-tagged at the amino (His_6-EloA) and carboxy (EloA-His_6) termini were constructed and the activities of the resulting fusion proteins were examined by GC/MS analysis of FAMEs prepared from total yeast lipids. As performed previously, the production of $18:1^{\Delta 11}$ as a percentage of the total FAMEs was reported (Figure 3.4). The results showed that the His_6-EloA enzyme had within 2% of the wild-type activity, while the EloA-His_6 enzyme was 19.5% less active than wild-type EloA.

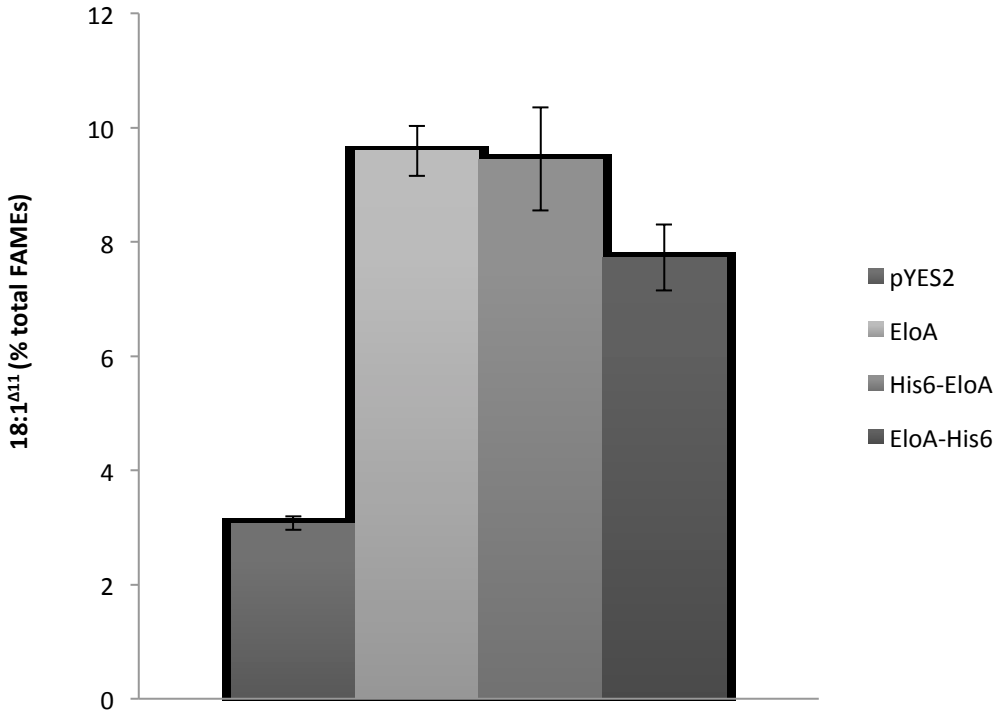

Figure 3.4. Production of $18:1^{\Delta 11}$ by pYES2, EloA, His_6-EloA, and EloA- His_6 upon expression in *S. cerevisiae*. $18:1^{\Delta 11}$ composition is represented as mean percent of total FAMEs ± sd (n=5 or 4). Wild-type and tagged protein were expressed from pYES2 (Invitrogen).

These results demonstrate differences in activity between the tagged and wild-type EloA that may be attributed to the impact of the hexahistidine tag on the stability of the structure of the protein. Once again these results were from *in vivo* experiments, and not assays of purified enzymes; therefore, yeast microsomes expressing the tagged proteins were prepared and protein expression levels analyzed by immunoblotting. Immunobloting analysis showed that protein staining in microsomes prepared from yeast transformed with the His_6-EloA-containing plasmid was significantly less than that seen with the wild-type gene (Figure 3.5). However, no staining with the anti-EloA sera was observed for the EloA-His_6 protein (Figure 3.6), potentially due to low expression levels or the placement of the tag interfering with the antibody.

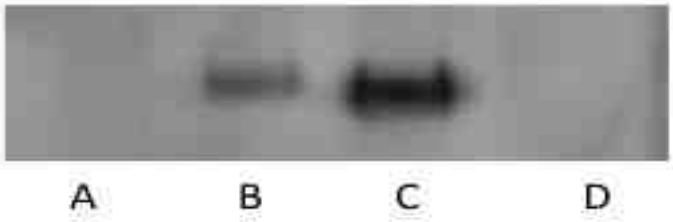

Figure 3.5. Immunoblot analysis of microsomes from yeast cells expressing tagged EloA. Microsomal protein (20 µg) was analyzed by immunoblot with anti-EloA. The immunoblot shows empty vector pYES2 (A), His_6-EloA subcloned into pYES2 B), EloA subcloned into pESc (C), and empty vector pESc (D) . Wild-type EloA is 32.2 kDa and His_6-EloA 33.1 kDa

Figure 3.6 shows an attempt to determine the expression levels of both the tagged fusion proteins along with the wild-type subcloned into the pYES2 expression vector to allow for comparisons of staining between the wild-type and the tagged fusion protein. Unfortunately, in this experiment no staining with the anti-EloA sera was observed for the EloA-His_6 protein or for the wild-type. Based on these results, it was determined that the best option for the isolation/solubilization assays would be the His_6-EloA as it showed wild-type like activity and immunoblot experiments showed staining for the tagged protein (Figure 3.5).

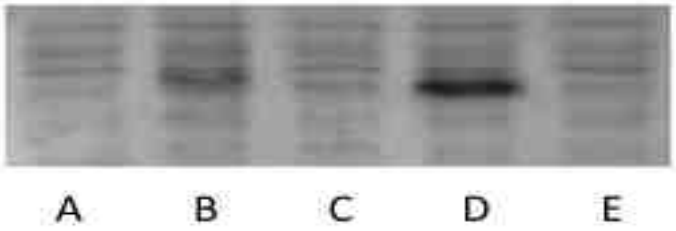

Figure 3.6. Immunoblot analysis of microsomes from yeast cells expressing tagged EloA. Microsomal protein (20 μg) was analyzed by immunoblot with anti-EloA. Immunoblot shows EloA-His_6 in pYES2 (A), His_6-EloA in pYES2 (B), EloA in pYES2 (C), EloA in pESc (D), and empty vector pYES2 (E).

The next step was to explore the optimal conditions for the solubilization and isolation of the membrane-bound EloA. Optimization of solubilization conditions was conducted using yeast microsomes expressing EloA or empty vector, pESc. The non-tagged protein was used to determine solubilization conditions before moving to the solubilization of the tagged protein because of the difficulty in immunoblot detection of the tagged fusion proteins.

Yeast microsomes expressing EloA or empty vector were prepared as previously described and treated with different concentrations of Triton X-100 to determine the optimal detergent concentration for EloA solubilization (Figure 3.7). The range of Triton X-100 concentrations tested were from 10-fold above to below the critical micelle concentration (CMC) of Triton X-100 of ~0.02% (w/v) (52).

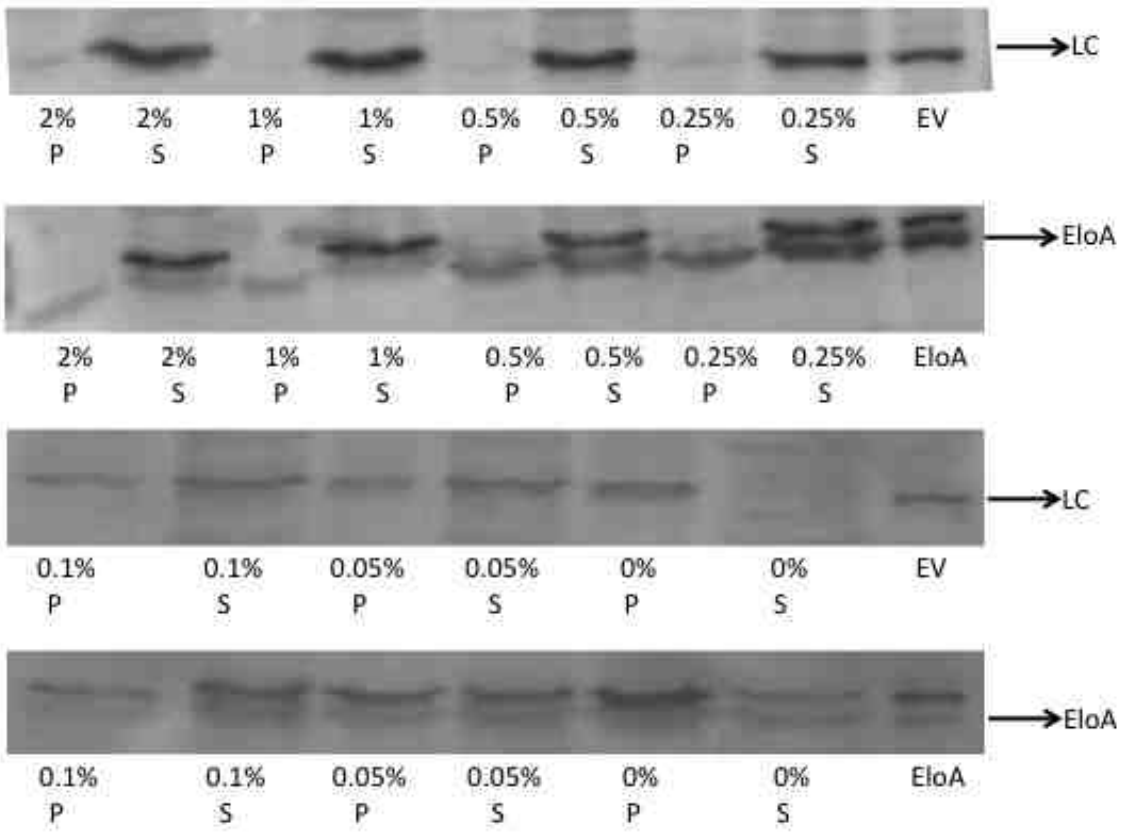

Figure 3.7. Optimization of solubilization conditions for EloA. Microsomes from yeast expressing EloA or pESc were prepared as described previously. Microsomes were treated with 320 mM NaCl and various percentages of Triton X-100 (0-2% (v/v)) followed by incubation on ice for 2 h and centrifugation to pellet insoluble material. Wild-type (EloA) and empty vector (pESc) (30 µl supernatant, S, or 30 µl pellet resuspension, P) were analyzed by immunoblot probed with anti-EloA and anti-Erg 27 and the chemiluminescent signal collected for 2 min. First lane from right to left shows untreated microsomes samples prepared as stated.

Immunoblotting of the soluble (supernatant) and insoluble (pellet) fractions showed that at the higher concentration of Triton X-100 (2%, Figure 3.7), most of EloA was found in the supernatant but this could suggest that the sample is saturated with the detergent. Additionally, 2% Triton X-100 is efficient but ten times more the CMC of Triton X-100. Furthermore, when Triton X-100 was excluded from the reaction, most of the protein in both the wild-type and empty vector samples, remained in the pellet suggesting that no solubilization of Erg27p or EloA had occurred. The concentrations of Triton X-100 tested were between 2 and 0.25% (v/v) and showed equivalent protein levels in both the pellet and the supernatant, disqualifying them as potential candidates for solubilization. At 0.05%, equivalent protein levels in both pellet and supernatant were observed.

The results showed that the optimal detergent concentration for solubilization of EloA was 0.1% Triton X-100 (Figure 3.7). At this Triton X-100 concentration, the pellet sample of the EloA microsomes showed little EloA staining while the supernatant sample showed substantial EloA staining suggesting that most of the protein remained in the supernatant of the sample. The conditions determined in this experiment were used to solubilize microsomes expressing the tagged protein and pYES2 empty vector.

In an attempt to isolate solubilized His_6-EloA, supernatants from the solubilization reactions were applied to both a nickel and a cobalt column. The empty vector sample was also subjected to metal-affinity chromatography to determine if endogenous proteins were isolated with the column used; this served as a negative control for the isolation

experiment. The activity of microsomes, solubilized microsomes, and eluates from Ni^2 and Co^{2+} affinity chromatography of supernatants from His_6-EloA and mock (EV) solubilization samples were monitored by a condensation assay, where the protein samples were incubated with an excess of radiolabeled substrate [2-^{14}C] malonyl-CoA, and 16:1-CoA in a sodium phosphate buffer with 0.1% Triton X-100. The 3-ketoacyl-CoA condensation products were reduced to the diols, extracted, and subjected to liquid scintillation counting to monitor the reaction.

Results (Figure 3.8) showed a decrease in radiolabeled material in the extracted products of the eluates compared to the microsomes suggesting that the activity of EloA was greatest in the microsomes when compared to the eluates. A possible reason for this outcome is that the condensation assay measured the substrate not the product extraction allowing for the observed decrease in counts. Another reason for the decrease in counts may be that the extraction of the diols was not efficient. Additionally, the condensation assay was conducted with equivalent sample volumes, not equivalent protein concentrations and it is thus possible that the amount of protein in the assayed samples could have varied. The observed results are likely due to a combination of nonequivalent protein concentrations and the extraction measuring the extracted diols and not the elongation product.

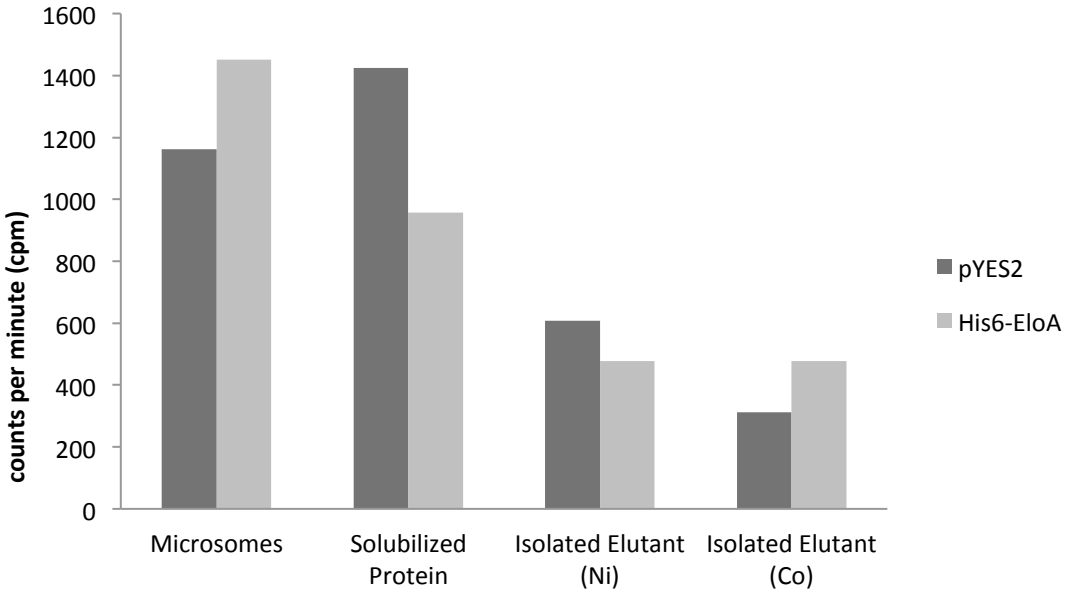

Figure 3.8. Condensation assay monitoring enzyme activity. Samples from empty vector (pYES2) and His_6-EloA were isolated with a nickel or a cobalt column. Samples (5 µl) were mixed with 15 mM [2-^{14}C] malonyl-CoA, 10 mM sodium phosphate, pH 7.2, 0.05% Triton X-100, 20 µM 16:1-CoA.

CHAPTER 4. DISCUSSION

4.1 Site-directed Mutagenesis of Highly Conserved Residues in EloA

ELOs are found in many organisms, including mammals, plants, protists, and fungi and have been shown to catalyze the condensation reaction of fatty acid elongation leading to the production of crucial fatty acids for many organisms. The unique characteristics of this enzyme, such as not having a conserved catalytic triad, suggest that these enzymes carry out the condensation reaction using novel chemistry. An understanding of the mechanism of these enzymes may impact the understanding and treatment of diseases such as Stargardt disease (8). Although the mechanism by which ELOs catalyze the condensation reaction during fatty acid elongation has not been elucidated, we reasoned that the highly conserved amino acid residues targeted in this study are likely to have a structural and/or a catalytic role in ELO function. Interest in the possible roles of these highly conserved residues led to the preparation of twenty individual EloA site-directed mutants.

Analysis of EloA mutants revealed significant roles for some residues in the structure or the catalytic function of EloA. In order to study the possible roles of the targeted residues, mutants were analyzed by quantifying the amount of EloA elongation product, $18{:}1^{\Delta 11}$%, from total FAMEs prepared from yeast expressing mutant EloA, EV, or wild-type followed by immunoblotting of microsomes prepared from yeast expressing

mutant alleles to determine levels of EloA expression. Three categories of mutants were observed; those within 20% of wild-type activity; those with between 10 and 60% of wild-type activity; and those with little or no activity. Immunoblotting results showed that most mutants have comparable EloA protein expression levels when compared to the wild-type suggesting that changes in activity were due to mutation disruptions and not low protein expression levels.

Analysis of highly conserved aromatic residues by site-directed mutagenesis demonstrated a structural role rather than a catalytic role. Tyr45 and Tyr181, highly conserved residues in the ELO family, were replaced with both alanine and phenylalanine residues. The alanine mutations were installed to examine whether the aromatic ring found at these two positions is necessary for a stable, active enzyme while phenylalanine mutations tested the necessity of the hydroxyl group for the native structure and/or activity of the enzyme. In both cases, the alanine mutants (Y45A and Y181A) were considerable less active than the wild-type enzyme while the phenylalanine mutants showed near wild-type activity, suggesting that there is a structural requirement for the aromatic ring while the phenolic group is not necessary to maintain an active enzyme. These results are consistent with the observation that a number of the ELOs have a phenylalanine or tryptophan residue at the position equivalent to Y45 in EloA and suggest that these residues may play a similar structural role as the tyrosine of EloA (12).

Claisen-like condensing enzymes have a catalytic triad (CHH/N) that is essential for catalysis. The cysteine residue found in the catalytic triad is thought to covalently bind the acyl primer prior to condensation with the malonyl-CoA-derived C_2 unit (11, 26). The sequence alignment of the functionally characterized ELOs (Figure 1.6) showed that the ELO family does not have an absolutely conserved cysteine residue; C104 of EloA is the only cysteine that is somewhat conserved (30% of sequences) in the family. When assayed, the C104A mutation resulted in an active enzyme retaining 68% of the wild-type activity and indicating that this residue is not essential for condensation activity. Additionally, the model for EloA membrane topology (Figure 1.7) (17) places C104 in a loop found on the luminal side of the ER membrane, away from the cytosol where the acyl-CoA and malonyl-CoA substrates of the enzyme are found. Thus, ELOs do not appear to covalently bind the acyl primer through a cysteine moiety, as there is no other conserved cysteine in the family.

If the substrate acyl group is covalently bound in the EloA active site, it may be through an ester linkage with a serine, threonine, or tyrosine residue. Two threonine residues (T130 and T200), modeled to be near the cytosol, were found to be important for activity (mutation to alanine resulted in 31% and 36% of wild-type activity, respectively). However, the stability of an ester linkage relative to a thiol ester linkage may make the subsequent condensation reaction less likely if the acyl group were bound through a hydroxyl side chain (53). Alternatively, the acyl primer may not be covalently bound at all, implying that the active site binds two CoA-bound substrates at the same time.

The histidine box (LHXXHH; residues 143-148 in EloA) found in the ELO family is the only primary structural motif found in ELOs with an easily identifiable similarity to motifs found in other enzymes. This motif is found in enzymes that catalyze oxidative reactions such as the fatty acid desaturases where it is essential and thought to bind the catalytic di-iron center (42). A variation of the histidine box, where the first histidine is replaced with a glutamine (LQXXHH) is found in "front-end" fatty acid desaturases, such as the Δ^6 desaturase from borage (54) that installs double bonds in fatty acids between the carbonyl group and an existing point of unsaturation at the Δ^9 position, and in ELO homologs from *Mortierella alpina* (MALCE1p) and microalgae (*Isochrysis galbana*; IgASE1) (55, 56).

The possible role of the conserved residues in the histidine box of EloA was probed: the mutation of H147 and H148 to alanine each abrogated EloA-catalyzed elongation activity (Figure 3.2) but had little effect on the protein level (Figure 3.3) while the H144A mutation maintained nearly 100% of the wild-type activity. An imidazole group at position 144 is, therefore, not necessary for EloA activity but H147 and H148 are each important for EloA activity suggesting a possible role in catalysis and/or structure. These results are consistent with those reported by Denic and Weismann who showed that a mutation of the second histidine in the histidine box of *S. cerevisiae* Elo2p (that corresponding to H147 of EloA) to alanine resulted in an inactive enzyme (41). Mutagenesis of the variant histidine box found in the *I. galbana* IgASE1 ELO (55) where the glutamine residue replacing the first histidine of the canonical histidine box was changed to either a histidine or an alanine, decreased activity but did not inactivate the

enzyme (57) while similar changes in the borage front-end desaturases abrogated activity (54, 58). Together these results indicate that the histidine box in the ELO family plays a different role than that in the desaturases and that there is a possibility that metal ions are not involved in the mechanism of the enzyme.

The mutation of many residues that are predicted to reside at the cytosolic side of the ER membrane (Figure 1.7) (17, 41) from polar residues (K123, D129, N173, H177, Q203, Q206) to alanine, resulted in the inactivation of EloA (Figure 3.2). As the acyl-CoA and malonyl CoA substrates of the enzyme are found in the cytosol, these results suggest a possible role of these residues in either substrate binding or in catalysis. The coenzyme A carrier of the acyl and malonyl groups is negatively charged suggesting that the positively charged residues (K123 and potentially H147, H148, H177) form salt bridges with the substrates.

Interestingly, residues with apparent roles in discriminating among acyl substrates of different lengths are found at the lumen proximal end of ELO transmembrane domains and have been suggested to limit the length of the acyl chain accepted by a particular ELO (41, 59). These studies, together with the findings of this study, strongly suggest that the acyl substrate enters a binding pocket within the membrane-spanning fold of the ELO with the methyl end leading and spanning the membrane while the carboxyl end is held at the cytosolic face where it is available for the condensation reaction with malonyl-CoA.

Site-directed mutagenesis of highly conserved residues in *D. discoideum* EloA has provided insight into residues possibly involved in catalyzing the condensation reaction (Table 4.1) in ELOs. It appears that the mechanism proceeds by a different pathway than that seen in fatty acid synthases, the related 3-ketoacyl-CoA synthases found in plants, and the polyketide synthases.

Table 4.1. Targeted highly and absolutely conserved amino acids in EloA, respective mutations and conclusions.

Target residue	**Mutation**	**Conclusion**
Tyrosine (Y45)	Alanine	phenyl group needed for active enzyme
Tyrosine (Y45)	Phenylalanine	maintained near wild-type activity; OH not needed for active enzyme
Serine (S79)	Alanine	within 20% wild-type activity
Cysteine (C104)	Alanine	68% wild-type activity, not part of catalytic triad
Lysine (K123)	Alanine	little to no activity, could be forming ionic bonds or salt bridges with primer
Glutamic acid (E126)	Alanine	between 10-60% wild-type activity
Aspartic acid (D129)	Alanine	little to no activity
Threonine (T130)	Alanine	little to no activity
Histidine (H144)	Alanine	near wild-type activity
Histidine (H147)	Alanine	little to no activity
Histidine (H148)	Alanine	little to no activity
Asparagine (N173)	Alanine	little to no activity
Histidine (H177)	Alanine	little to no activity
Methionine (M180)	Alanine	between 10-60% wild-type activity
Tyrosine (Y181)	Alanine	phenyl group needed for active enzyme
Tyrosine (Y181)	Phenylalanine	maintained near wild-type activity; OH not needed for active enzyme
Threonine (T200)	Alanine	between 10-60% wild-type activity
Glutamine (Q203)	Alanine	little to no activity
Glutamine (Q206)	Alanine	little to no activity
Phenylalanine (F252)	Alanine	little to no activity

4.2 Preliminary Work Towards the Isolation of EloA

In order to explore in more depth the mechanism by which ELOs catalyze the condensation reaction, it is essential to obtain purified enzyme. Attempts to isolate EloA were conducted and began with the construction of expression plasmids for EloA separately hexahistidine-tagged at its amino (His_6-EloA) and carboxyl (EloA-His_6) termini. The activity of the tagged protein was analyzed by preparing FAMEs from total yeast lipids and analyzed by GC/MS as previously performed by Blacklock et al. when isolating KCSs (15). The production of $18:1^{\Delta 11}$ as a percentage of the total FAMEs was determined (Figure 3.4) and demonstrated that the His_6-EloA was within 2% wild-type activity while the EloA-His_6 plasmid was somewhat less active (19.5%) than wild-type EloA. Based on these results, it was determined that the His_6-EloA protein was the best candidate for our solubilization and isolation experiments. In order to purify the enzyme, microsomes prepared from yeast expressing the tagged protein were solubilized and subjected to metal affinity chromatography to isolate the tagged protein.

Here, we showed that the optimal detergent concentration for solubilization of EloA was 0.1% Triton X-100, which is ten times higher than the CMC of the detergent. The optimal concentration of Triton X-100 was determined by selecting a range of detergent concentrations above and below the CMC. The optimal percentage of Triton X-100 determined in our experiment was comparable to percentages of Triton X-100 used in isolation experiments reported previously (60).

Metal-affinity isolation of His_6-EloA was attempted using two different columns: Ni-NTA and Talon-Co affinity resin. Preliminary results (Figure 3.8) were uncertain, as we are not aware of the state (properly folded or disrupted by the isolation experiment) of the eluted protein.

Possible reasons for the observed results include the metal-affinity chromatography used; the experiment tested two columns but the results obtained were similar between the Ni and Co columns. Additionally, as previously mentioned, the condensation assay measures the extracted formed diols not the elongation product making it difficult to quantify the activity of the enzyme. Finally, there is a possibility that the enzyme was isolated by metal-affinity chromatography but it was inactive by the time it was assayed. Solutions for these problems include immunoblotting fractions collected from the column to determine at what point during the isolation the eluate contains the most protein and test by fraction with the most eluted protein by the condensation assay.

Due to the membrane-bound nature of the protein of interest, other avenues must be pursued to determine optimal isolation conditions. Small-sized tags in addition to the hexahistidine tag are available for protein purification, such as the polyarginine tag, FLAG tag (DYKDDDDK), c-myc tag (EQKLISEEDL), Strep II tag (WSHPQFEK) and S tag (KETAAAKFERQHMDS). Another way to purify proteins includes the use of large peptides (26-396 residues); however, with an increasing size of the tag there is a larger risk of the tag interfering with protein-protein interactions (61). The solubility can increase while tagged but the tag must be removed for certain experiments such as the

production of an antibody and crystallization of the protein (60, 61). Additionally, many parameters, including effects on tertiary structure, pH, yield, purity, and cost (62) must be considered when choosing an affinity tag.

A previously published study using a strep II tag placed at the amino or carboxy termini of a membrane-bound cytochrome P450 demonstrated an alternative method to successfully isolate a protein of interest (60). The strep II tag-containing plasmid was expressed in *S. cerevisiae* and microsomes were isolated. The microsomes were solubilized with a similar protocol and using the same percentage of Triton X-100 (0.1%) as those described in this study. The use of the strep II tag at either the amino or carboxy termini resulted in the successful isolation with a *Strep*-Tactin® column of the membrane-bound protein in its active form (60).

Similarly, other studies show the successful isolation of an active ELOs using a FLAG tag (41). The ELOs analyzed by Denic and Weissman were tagged at the C-terminus and expressed in yeast. Proteins were solubilized using either 1% Triton X-100 or 2% digitonin and isolated by immunoprecipitation using an anti-FLAG resin. The purified protein was reconstituted into proteoliposomes by detergent removal using SM2 Bio-Beads in the presence of synthetic phospholipids. Proteoliposomes were used for immonoblotting exeperiments. A radiolabeled experiment using reverse-phase TLC was utilized to monitor the elongation activity of the enzyme by analyzing the reaction products (41).

Future experiments could include attempting to isolate EloA using the methodology reported by Denic and Weissman, which was similar to the methods utilized here but differed in the amount of detergent (1% used by Denic and Weissman vs. 0.1% used in this study), the method of isolating, and the purified protein activity assay.

Although previous studies have reported the successful isolation of active membrane-bound proteins, the isolation of active EloA was not achieved in this study. Future studies of the purification of membrane-bound EloA require the testing of different affinity tags, a higher detergent concentration, and improvements on the assays conducted to assay the activity of the isolated enzyme. For example, EloA could be tagged with FLAG and immunoprecipitation could be used to isolate protein from microsomes prepared from yeast expressing EloA followed by reconstitution of purified protein into proteoliposomes. Once the active form of EloA has been isolated, the mutants created can be assayed to determine if the residues have a role in the individual steps of the condensation reaction and determine what these steps might be in the condensation mechanism of ELOs.

Further, the isolation of active EloA could allow the crystallization of the protein and a better model. Furthermore, the highly conserved residues could be mutated to residues with similar characteristics. Mutating residues to similar amino acids could provide insights into their role in the condensation mechanism.

For example, mutating K123 to an arginine residue maintaining the positive charge or changing it to a negatively charged residue to test the effects if the side chain participates in the anchoring the substrate.

Knowing how ELOs behave mechanistically can benefit research on human diseases, as previously mentioned mutations of ELOs are known to lead human disease. Another example is *Trypanosoma brucei*'s Elop homologs instructing the synthesis of short fatty acids that are important during the parasite's invasion of a host's immune system (63), other ELOs could have similar roles. Understanding how ELOs behave can lead to drug development or therapeutic design for diseases such as adrenoleukodystrophy (ALD) which is a neurodegenerative disease due to demyelination of the nervous system caused by overproduction of C26 saturated fatty acids *(*64). Overall, the findings reported here led to a better understanding of the mechanistic behavior of ELOs through the analysis of site-directed EloA mutants. Our findings should serve as a stepping-stone for the isolation of EloA.

REFERENCES

REFERENCES

1. Vance, D. E., Vance, J. E. (2008) *Biochemistry of Lipids, Lipoproteins and Membranes, 5th Edition*, Elsevier.
2. Voet, D., Voet, J. G. (1995) *Biochemistry*, Vol. 2, John Wiley & Sons, Inc.
3. Schweizer, M. (2004) *Metabolism and Molecular Physiology of Saccharomyces Cerevisiae, 2nd Edition*, CRC Press.
4. Schneiter, R., Brugger, B., Ammann, C. M., Prestwich, G. D., Epand, R. F., Zellnig, G., Wieland, F. T., Epand, R. M. (2004) Identification and biophysical characterization of a very-long-chain-fatty-acid-substituted phosphatidylinositol in yeast subcellular membranes, *Biochemistry 381*, 941-949.
5. Poulos, A. (1995) Very Long Chain Fatty Acids in Higher Animals-A Review, *Lipids 30*.
6. Samuels, L., Kunst, L., Jetter, R. (2008) Sealing Plant Surfaces: Cuticular Wax Formation by Epidermal Cells, *Annu. Rev. Plant Biol. 59*, 683-707.
7. Millar, A. A., Kunst, L. (1997) Very-long-chain fatty acid biosynthesis is controlled through the expression and specificity of the condensing enzyme, *Plant J. 12*, 121-131.
8. McMahon, A., Butovich, I. A., Mata, N. L, Klein, M., Ritter III, R., Richardson, J., Birch, D. G., Edwards, A. O., Kedzierski, W. . (2007) Retinal Pathology and skin barrier defect in mice carrying a Stargardt disease-3 mutation in elongase of very long chain fatty acids-4, *Mol Vis 13*, 258-272.
9. Qi, B., Fraser, T., Mugford, S., Dobson, G., Sayanova, O., Butler, J., Napier, J. A., Stobart, A. K., Lazarus, C. (2004) Production of very long chain polyunsaturated omega-3 and omega-6 fatty acids in plants, *Nat Biotechnol 22*.
10. Haslam, T. M., Kunst, L. (2013) Extending the story of very-long-chain fatty acid elongation, *Plant Sci 210*, 93-107.
11. Heath, R. J., Rock, C. O. (2002) The Claisen condensation in biology, *Nat. Prod. Rep. 19*, 581-596.
12. Hernandez-Buquer, S., Blacklock, B. J. (2013) Site-directed mutagenesis of a fatty acid elongase ELO-like condensing enzyme, *FEBS Lett.*
13. Tehlivets, O., Scheuringer, K., Kohlwein, S. D. (2007) Fatty acid synthesis and elongation in yeast, *Biochimi Biophys Acta*, 255-270.
14. Blacklock, B. J., Jaworski, J.G. (2002) Studies into factors contributing to substrate specificity of membrane-bound 3-ketoacyl-CoA synthases, *Eur. J. of Biochem 269*, 4789-4798.
15. Blacklock, B. J., Jaworski, J. G. (2006) Substrate specificity of Arabidopsis 3-ketoacyl-CoA synthases, *Biochem Bioph Res Co 346*, 583-590.

16. Oh, C. S., Toke, D. A., Mandala, S., Martin, C. E. (1997) ELO2 and ELO3, homologs of the Saccharomyces cerevisiae ELO1 gene, function in fatty acid elongation and are required for sphingolipid formation, *J. Biol. Chem. 272*, 17376-17384.
17. Blacklock, B. J., Kelley, D., Patel, S. (2008) A fatty acid elongase ELO with novel activity from *Dictyostelium discoideum*, *Biochem. Biophys. Res. Commun. 374*, 226-230.
18. Toke, D. A., Martin, C. E. (1996) Isolation and characterization of a gene affecting fatty acid elongation in Saccharomyces cerevisiae, *J. Biol. Chem. 271*, 18413-18422.
19. Qi, B., Beaudoin, F., Fraser, T., Stobart, A. K., Napier, J. A., Lazarus, C. (2002) Identification of a cDNA encoding a novel C18-9 polyunsaturated fatty acid-specific elongating activity from the docosahexaenoic acid (DHA)-producing microalga, Isochrysis galbana, *FEBS Lett.*, 159-165.
20. Quist, T. M., Sokolchik, I., Shi, H., Joly, R. J., Bressan, R. A., Maggio, A., Narsimhan, M., Li, X. (2009) HOS3, an ELO-like gene, inhibits effects of ABA and implicates a S-1-P/ceremide control system for abiotic stress responses in Arabidopsis thaliana, *Mol. Plant*, 138-151.
21. Todd, J., Post-Beittenmiller, D., Jaworski, J. G. (1999) KCS1 encodes a fatty acid elongase 3-ketoacyl-CoA synthase affecting wax biosynthesis in Arabidopsis thaliana, *Plant J.*, 119-130.
22. James, D. W., Lim, E., Keller, J., Plooy, I., Ralston, E., Dooner, H. K. (1995) Directed tagging of the Arabidopsis FATTY ACID ELONGATION1 (FAE1) gene with the maize transposon Activator, *Plant Cell*, 301-319.
23. Venkateswari, J., Kanrar, S., Kirti, P.B., Malathi, V. G., Chopra, V. L. (1999) Molecular cloning and characterization of FATTY ACID ELONGATION1 (BjFAE1) gene of Brassica juncea, *J. Plant Biochem. Biotech*, 53-55.
24. Kim, J., Jung, J. H., Lee, S. B., Go, Y. S., Kim, H. J., Cahoon, R., Markham, J. E., Cahoon, E., Suh, M.C. (2013) Arabidopsis 3-ketoacyl-CoA synthase 9 is involved in the synthesis of tetracosanoic acids as precursors of cuticular waxes, suberins, sphingolipids, and phospholipids, *Plant Physiol.*, 567-580.
25. Venegas-Caleron, M., Beaudoin, F., Sayanova, O., Napier, J.A. (2007) Co-transcribed genes for long chain polyunsaturated fatty acid biosynthesis in the protozoon Perkinsus marinus include a plant-like 3-ketoacyl coenzyme A synthase, *J. Biol. Chem.*, 2996-3003.
26. Ghanaveti, M., Jaworski, J. G. (2001) Active-site residues of a plant membrane-bound fatty acid elongase B-ketoacyl-CoA synthase, FAE 1 KCS, *Biochim. Biophys. Acta. 1530*, 77-85.
27. Ghanaveti, M., Jaworski, J. G. (2002) Engineering and mechanistic studies of the Arabidopsis FAE 1 b-ketoacyl-CoA synthase, FAE 1 KCS, *Eur. J. Biochem 269*, 3531-3539.
28. B. J. Blacklock, D. K., S. Patel. (2008) A fatty acid elongase ELO with novel activity from Dictyostelium discoideum *Biochem. Biophys. Res. Commun.*, 226-230.

29. Kajikawa, M., Yamato, K.T., Sakai, Y., Fukuzawa, H., Ohyama, K., Kohchi, T. (2006) Isolation and functional characterization of fatty acid 5-elongase gene from the liverwort Marchantia polymorpha L, *FEBS Lett.*, 149-154.
30. Meyer, A., Kirsch, H., Domergue, F., Abbadi, A., Sperling, P., Bauer, J., Cirpus, P., Zank, T. K., Moreau, H., Roscoe, T. J, Zahringer, U., Heinz, E. (2004) Novel fatty acid elongases and their use for the reconstitution of docosahexaenoic acid biosynthesis, *J. Lipid Res.*, 1899-1909.
31. El-Sherbeini, M., Clemas, J. (1995) Cloning and characterization of GNS1: a Saccharomyces cerevisiae gene involved in synthesis of 1,3-beta-glucan in vitro, *J. Bacteriol*, 3227-3234.
32. Garcia-Arranz, M., Maldonado, A. M., Mazon, M. J., Portillo, F. (1994) Transcriptional control of yeast plasma membrane H+-ATPase by glucose., *J. Biol. Chem. 269*, 18076-18082.
33. Zank, T. K., Zähringer, U., Beckmann, C., Pohnert, G., Boland, W., Holtorf, H., Reski, R., Lerchi, J., and Heinz, E. (2002) Cloning and functional characterisation of an enzyme involved in the elongation of Delta6-polyunsaturated fatty acids from the moss *Physcomitrella patens*, *Plant J. 31*, 255-268.
34. Zhang, K. M., Kniazeva, M., Han, M., Li, W., Yu, Z., Yang, Z., Li, Y., Metzker, M. L., Allikmets, R., Zack, D. J., Kakuk, L. E., Lagali, P. S., Wong, P. W., MacDonald, I. M., Sieving, P.A., Figueroa, D. J., Austin, C. P., Gould, R. J., Ayyagari, R., and Petrukhin, K. (2001) A 5-bp deletion is ELOVL4 is associated with two related forms of autosomal dominant macular dystrophy, *Nat. Genet.* , 89-93.
35. Raz-Prag, D., Ayyagari, R., Fariss, R. N., Mandal, M. N. A., Vasireddy, V., Majchrzak, S., Webber, A. L., Bush, R. A., Salem, N., Petrukhin, K., and Sieving, P.A. (2006) Haploinsufficiency is not the key mechanism of phatogenesis is a heterozygous Elovl4 knockout mouse model of STGD3 disease, *Invest. Ophthalmol. Vis. Sci. 47*, 3603-3611.
36. Cameron, D. J., Tong, Z., Yang, Z., Kaminoh, J., Kamiyah, S., Chen, H., Zeng, J., Chen, Y., Luo, L., and Zhang K. (2007) Essential role of Elovl4 in very long chain fatty acid synthesis, skin permeability barrier function, and neonatal survival, *Int. J. Biol. Sci 3*, 111-119.
37. Jorgensen, J. A., Zadravec, D., and Jacobsson, A. (2001) Norepineprine and rosiglitazone synergistically include Elovl3 expression in brown adipocytes, *Am. J. Physiol. Endocrinol. 293*, E1159-E1168.
38. Zadravec, D., Brolinson, A., Fisher, R. M., Carneheim, C., Csikasz, R. I., Bertrand-Michel, J., Boren, J., Guillou, H., Rudling, M., and Jacobsson, A. (2010) Ablation of the very-long-chain fatty acid elongase ELOVL3 in mice leads to constrained lipid storage and resistance to diet-induced obesity, *FASEB J. 24*, 4366-4377.
39. Zadravec, D., Tvrdik, P., Guillou, H., Haslam, R., Kobayashi, T., Napier, J. A., Capecchi, M. R., and Jacobbson A. (2011) ELOVL2 controls the level of n-6 28:5 and 30:5 fatty acids in testis, a prerequisite for male fertility and sperm maturation in mice, *J. LIpid Res. 52*, 245-255.

40. Hashimoto, K., Yoshizawa A. C., Okuda, S., Kuma, K., Goto, S., Kanehisa, M. (2008) The repertoire of desaturases and elongases reveals fatty acid variations in 56 eukaryotic genomes, *J. Lipid Res. 49*, 183-191.
41. Denic, V., Weissman, J. S. (2007) A molecular caliper mechanism for determining very long-chain fatty acid length, *Cell 130*, 663-677.
42. Shanklin, J., Whittle, E., Fox, B. G. (1994) Eight histidine residues are catalytically essential in a membrane-associated iron enzyme, steaoyl-CoA desaturase, and are conserved in alkane hydroxylase and xylene monooxygenase, *Biochemistry 33*, 12787-12794.
43. Elchinger, L., Pachebat, J. A., Glockner, G., Rajandream, M.-A., Sucgang, R., Berriman, M., Song, J., Olsen, R., Szafranski, K., Xu, Q., Tunggal, B., Kummerfeld, S., Madera, M., Konfortov, B. A., Rivero, F., Bankler, T. A., Lehmann, R., Hamlin, N., Davies, R., Gaudet, P., Fey, P., Plicher, K., Chen, G., Saunders, D., Sodergren, E., Davis, P., Kerhornou, A., Nie, X., Hall, N., Anjard, C., Hemphill, L., Bason, N., Farbrother, P., Desany, B., Just, E., Morio, T., Rost, R., Churcher, C., Cooper, J., Haydock, S., van Driessche, N., Cronin, A., Goodhead, I., Muzny, D., Mourier, T., Pain, A., Lu, M., Harper, D., Lindsay, R., Hauser, H., James, K., Quiles, M., Madan Babu, M., Salto, T., Buchrieser, C., Wardroper, A., Felder, M., Thangavelu, M., Johnson, D., Knights, A., Loulseged, H., Mungall, K., Oliver, K., Price, C., Quail, M. A., Urushihara, H., Hernandez, J., Rabbinowitsch, E., Steffen, D., Sanders, M., Ma, J., Kohara, Y., Sharp, S., Simmonds, M., Spiegler, S., Tivey, A., Sugano, S., White, B., Walker, D., Woodward, J., Winckler, T., Tanaka, Y., Shaulsky, G., Schleicher, M., Weinstock, G., Rosenthal, A., Cox, E. C., Chisholm, R. L., Gibbs, R., Loomis, W. F., Platzer, M., Kay, R. R., Williams, J., Dear, P. H., Noegel, A. A., Barrell, B., Kuspa, A. (2005) The genome of the social amoeba Dictyostelium discoideum, *Nature 435*, 43-57.
44. Annesley, S. J., Chen, S., Francione, L. M., Sanislav, O., Chavan, A. J., Farah, C., De Piazza, S. W., Storey, C. L., Ilievska, J., Fernando, S. G., Smith, P. K., Lay, S. T., Fisher, P. R., . (2013) Dictyostelium, a microbial model for brain disease, *Biochim. Biophys. Acta.*
45. Escalante, R., Vicente, J. J. (2000) Dictyostelium discoideum: a model system for differentiation and patterning., *Int. J. Dev. Biol.*, 819-835.
46. Insall, R. (2005) The Dictyostelium genome: the private life of a social model revealed?, *Genome Biol. 6*.
47. Hanahan, D. (1985) *Techniques for transformation of Escherichia coli. In DNA Cloning: a practical approach.* , Vol. 1, Oxford University Press.
48. Geitz, R. D., Woods, R. A. (2002) Transformation of yeast by lithium acetate/ single-stranded carrier DNA/polyethylene glycol method, *Methods Enzymol. 350*, 87-96.
49. Bradford, M. M. (1976) A rapid and sensitive method for the quantification of microgram quantities of protein utilizing the principle of protein-dye binding, *Analytical biochemistry*, 248-254.
50. Laemmli, U. K. (1970) Cleavage of structural proteins during the assembly of the head of bacteriophage T4, *Nature 227*, 680-685.

51. Taramino, S., Valachovic, M., Oliaro-Bosso, S., Viola, F., Teske, B., Bard, M., Balliano, G. (2010) Interactions of oxidosqualene cyclase (Erg7) with 3-keto reductase (Erg27) and other enzymes of sterol biosynthesis in yeast, *Biochim. Biophys. Acta. 1801*.
52. Scientific, T. Triton X-100 Detergent Solution, http://www.piercenet.com.
53. Jencks, W. P., Cordes, S., Carriuolo, J. (1960) The free energy of thiol ester hydrolysis, *J. Biol. Chem. 235*, 3608-3614.
54. Sayanova, O., Smith, M. A., Lapinskas, P., Stobart, A. K., Dobson, G., Christie, W. W., Shewry, P. R., Napier, J. A., . (1997) Expression of a borage desaturase cDNA containing an N-terminal cytochrome *b*5 domain results in the accumulation of high levels of Δ6-desaturase fatty acids in transgenic tabacco, *Proc. Natl Acad. Sci. USA 94*, 4211-4216.
55. Qi, B., Beaudoin, F., Fraser, T., Stobart, A. K., Napier, J. A., Lazarus, C. M. (2002) Identification of a cDNA encoding a novel C18-Δ9 polyunsaturated fatty acid-specific elongation activity from the docosahexaenoic acid (DHA)-producing microalga, *Isochrysis galbana*, *FEBS Lett. 510*, 159-165.
56. Sakuradani, E., Nojiri, M., Suzuki, H., Shimizu, S. (2009) Identification of a novel fatty acid elongase with a wide substrate specificity from arachidonic acid-producing fungus *Mortieralla alpina* 1S-4, *Appl. Microbiol. Biotech. 84*, 709-716.
57. Qi, B., . Fraser, T. C. M., Bleakley, C. L., Shaw, E. M., Stobart, A. K., Lazarus, C. M. (2003) The variant 'His-box' of the C18- 9-PUFA-specific elongase IgASE1 from Isochrysis galbana is essential for optimum enzyme activity, *FEBS Lett. 547*, 137-139.
58. Sayanova, O., Beaudoin, F., Libisch, B., Castel, A., Shewry, P. R., Napier, J. A. (2001) Mutagenesis and heterologous expression in yeast of a plant Δ6-fatty acid desaturase, *J. Exp. Bot. 52*, 1581-1585.
59. Vrinten, P. L., Hoffman, T., Bauer, J., Qui, X. (2010) Specific protein regions influence substrate specificity and product length in polyunsaturated fatty acid condensing enzymes, *Biochemistry 49*, 3879-3886.
60. Hamann, T., Laursen, T., Lindberg Moller, B. (2009) Functional expression of N-terminally tagged membrane boud cytochrome P450, *Protein Expres Purif 68*, 18-21.
61. Terpe, K. (2003) Overview of tag protein fusions: from molecular and biochemical fundamentals to commercial systerms, *Appl. Microbiol. Biotech. 60*, 523-533.
62. Lichty, J. J., Malecki, J. L., Agnew, H. D., Michelson-Horowitz, D. J., Tan, S. (2005) Comparison of affinity tags for protein purification, *Protein Expres Purif 41*, 98-105.
63. Lee, S. H., Stephens, J. L., Paul, K. S., and Englund, P. T. (2006) Fatty Acid Synthesis by Elongases in Trypanosomes, *Cell 126*, 691-699.
64. Kemp, S., Valianpour, F., Denis, S., Ofman, R., Sanders, R. J., Mooyer, P., Barth, P. G., Wanders, R. J. (2005) Elongation of very-long chain fatty acids is enhanced in X-linked adrenoleukodystrophy, *Mol Genet Metab*, 144-151.

APPENDIX

APPENDIX

Luria Broth (LB) plus ampicillin media/plates

Prepared the following in 500 ml nanopure H_2O and autoclaved at 15 psi for 20 min:

- 5g Tryptone
- 2.5g Bacto Yeast Extract
- 5g NaCl
- 7.5g Agar*
- 1 NaOH pellet*

*Ingredients added for LB + amp plates

Ampicillin (0.5 ml) was added after autoclave cool down.

SOC Broth

Prepared the following in 500 ml nanopure H_2O and autoclaved at 15 psi for 20 min:

- 10g Tryptone
- 2.5g Bacto Yeast Extract
- 10 mM NaCl
- 2.5 mM KCl
- 10 mM $MgCl_2$
- 10 mM $MgSO_4$

Complete minimal media-histidine/uracil plus dextrose plates: 450 mL volume.

Prepared the following in 450 mL nanopure H_2O and autoclaved at 15 psi for 20 min:

- 0.65g Dropout powder premix*
- 0.85g Yeast nitrogenous base w/o amino acids and ammonium sulfate
- 2.5g Ammonium sulfate
- 10g Dextrose
- 10g Agar
- 1 NaOH pellet

* Recipe obtained from Current Protocols in Molecular Biology Volume 2, 13.1

Complete minimal media-histidine/uracil: 450 mL volume.
Prepared the following in 450 mL nanopure H_2O and autoclaved at 15 psi for 20 min:

- 0.65g Dropout powder premix
- 0.85g Yeast nitrogenous base w/o amino acids and ammonium sulfate
- 2.5g Ammonium sulfate

YPAD media: 500 mL volume.
Prepared the following in 500 mL nanopure H_2O and autoclaved at 15 psi for 20 min:

- 5g Bacto yeast extract
- 10g Dextrose
- 10g Peptone
- 15mg Adenine Hemisulfate

12% Sodium Dodecyl Sulfate (SDS) polyacrylamide gels

- 2.4 mL 30% Acrylamide (29:1)
- 2.0 mL Sterile H_2O
- 30 µL 20% SDS
- 1.5 µL 1.5 M Tris pH 8.8
- 50 µL 10 % Ammonium persulfate (APS, made fresh)
- 5 µL Tretramethylethylenediamine (TEMED)

Added a layer of 0.01% SDS liquid and allowed to polymerized over night at 4 °C

Removed 0.01% SDS liquid layer and prepared stacking gel as follows:

- 0.25 mL 30% Acrylamide (29:1)
- 1.12 mL Sterile H_2O
- 9.5 µL 20% SDS
- 0.47 mL 0.5 M Tris pH 6.8
- 2.5 µL 10% APS (made fresh)
- 2.5 µL TEMED

*5X SDS Electrophoresis Buffer**

- 125 mM Tris-Cl, pH 8.3
- 960 mM Glycine
- 0.5% SDS
- H_2O to 1L

* Current Protocols in Molecular Biology Volume 2, 10.

Western Transfer Buffer

- 3 g Tris Base
- 14.4 g Glycine
- 200 ml Methanol
- H_2O to 1L

PUBLICATION

FEBS Letters 587 (2013) 3837–3842

ELSEVIER

FEBS Letters

journal homepage: www.FEBSLetters.org

Site-directed mutagenesis of a fatty acid elongase ELO-like condensing enzyme

Selene Hernandez-Buquer, Brenda J. Blacklock *

Department of Chemistry and Chemical Biology, Indiana University – Purdue University Indianapolis, Indianapolis, IN 46202, USA

ARTICLE INFO

Article history:
Received 9 September 2013
Revised 8 October 2013
Accepted 12 October 2013
Available online 21 October 2013

Edited by Miguel De la Rosa

Keywords:
Fatty acid elongation
Condensing enzyme
ELO

ABSTRACT

The condensation step of fatty acid elongation is the addition of a C_2 unit from malonyl-CoA to an acyl primer catalyzed by one of two families of enzymes, the 3-ketoacyl-CoA synthases and the ELO-like condensing enzymes. 3-Ketoacyl-CoA synthases use a Claisen-like reaction mechanism while the mechanism of the ELO-catalyzed condensation reaction is unknown. We have used site-directed mutagenesis of *Dictyostelium discoideum* EloA to identify residues important to catalytic activity and/or structure. Mutation of highly conserved polar residues to alanine resulted in an inactive enzyme strongly suggesting that these residues play a role in the condensation reaction.

1. Introduction

Very long-chain fatty acids (VLCFA), those fatty acids with chain lengths of C_{20} and greater, play pivotal roles in cellular structure and regulation. The acyl chains of ceramides and more complex sphingolipids, the building blocks of membrane microdomains, are often VLCFAs [1] and may be essential for the signaling function of sphingolipids [2]. The presence of VLCFAs in both leaflets of the lipid bilayer are thought to stabilize curved membranes [3]. Both land plants and animals exploit the hydrophobic nature of VLCFAs for protection against dehydration and the environment. In plants, VLCFA up to C_{32} are found as components of cuticular wax and suberin [4,5], while in mammals, VLCFAs longer than C_{30} are essential for the proper structure and function of the skin by creating a permeability barrier [6]. C_{22} VLCFAs are an important component of retinal lipids and C_{20} is a precursor of mediators involved in the inflammatory response [6,7].

VLCFA are produced at the ER membrane from de novo synthesized C_{16} and C_{18} fatty acids through the activity of a membrane-bound fatty acid elongase complex comprised of a condensing enzyme, two reductases, a dehydratase, and, as recently shown in plants, an immunophilin-like scaffolding protein [8,9]. Together, these independent polypeptides catalyze a series of reactions analogous to those catalyzed by fatty acid synthases in the condensation of a C_2-unit from malonyl-CoA with an acyl primer to form an elongated 3-ketoacyl-CoA, which is subsequently reduced to the enoyl-CoA, dehydrated, and further reduced to the product acyl-CoA.

Two families of fatty acid elongase condensing enzymes have been described. Animals, fungi, and other higher-order eukaryotes accomplish fatty acid elongation with a distinct family of condensing enzymes, first described in *Saccharomyces cerevisiae* as ELOs, which have been modeled to span the membrane five to seven times [10–14]. *Arabidopsis* also has predicted homologs to the ELOs; one, HOS3, is implicated in the production of C_{26} fatty acids that are incorporated into ceramides [15]. In plants and protists, 3-ketoacyl-CoA synthases (KCSs) with sequence similarities to the canonical Fatty Acid Elongase 1 KCS (FAE1 KCS) catalyze the initial step in fatty acid elongation and have apparent structural and catalytic similarities with the Type II fatty acid synthase condensing enzyme [8,16–20].

ELOs have substrate specificities that cover a wide range of fatty acid chain lengths and degrees of unsaturation and can be classified into phylogenetic clades based on their biochemically characterized activity with saturated and mono- or polyunsaturated substrates [10,21,22]. In yeast, Elo2p and Elo3p are responsible for the production of the saturated C_{26} acyl chains found in sphingolipids and a simultaneous disruption of the genes encoding these ELOs is synthetically lethal [12,13,23]. Lower plants and

Abbreviations: VLCFA, very long chain fatty acids; CoA, coenzyme A; KCS, 3-ketoacylCoA synthase; GC/MS, gas chromatography/mass spectrometry; ER, endoplasmic reticulum

* Corresponding author. Address: Department of Chemistry and Chemical Biology, Indiana University – Purdue University Indianapolis, 402 N. Blackford St., Indianapolis, IN 46202, USA.
E-mail address: bblacklo@iupui.edu (B.J. Blacklock).

0014-5793/$36.00
http://dx.doi.org/10.1016/j.febslet.2013.10.011

microalgae produce polyunsaturated VLCFA such as eicosapentaenoic acid and docosahexaenoic acid through the activities of ELOs and desaturases with distinct substrate specificities [24]. ELOs have been described in mammals where their functions are being unraveled. One, ELOVL4, is linked with a form of Stargardt disease, STGD3, the most common form of inherited macular dystrophy in which the macula atrophies and a degeneration of retinal pigment epithelium is observed [6]. Three alleles have been identified for STGD3, each of which results in a truncated protein that is missing the dilysine ER retention motif; the mislocalization of coexpressed mutant and wildtype ELOVL4 is thought to be the root of at least some of the phenotypic readout [25,26]. Disruption of both copies of ELOVL4 in mice results in a neonatal lethality where missing skin lipids results in the inability to retain water [11]. ELOVL3 appears to have roles in the synthesis of triacylglycerols in the liver and their accumulation in adipose tissue [27,28] while the very long chain polyunsaturated fatty acids produced by ELOVL2 are essential for spermatogenesis and male fertility [29].

Despite each catalyzing condensation reactions with identical substrates, ELOs and KCSs have no sequence or predicted topological similarity. Sequence alignment and mutagenesis have demonstrated that FAE1 KCS possesses a catalytic triad identical to those found in fatty acid synthase and polyketide synthase condensing enzymes (Cys His His/Asn) [30,31]. These enzymes catalyze the first step in elongation via a Claisen-like condensation [30,32] where the acyl-CoA substrate enters the active site first and, upon a nucleophilic substitution reaction, is covalently bound by the active site cysteine releasing the CoA moiety. The malonyl-CoA substrate then enters the active site and, either in a step-wise or concerted fashion, is decarboxylated and the generated enolate/carbanion, nucleophilically attacks the carbonyl group of the acyl primer, generating the 3-ketoacyl CoA product via an enzyme-bound tetrahedral intermediate [31].

ELOs have clearly been shown to independently catalyze the condensation of malonyl-CoA with an acyl-CoA in reconstituted proteoliposomes [33], however, the mechanism by which this reaction proceeds has not been delineated. There is no conserved Claisen-like condensing enzyme catalytic triad found in ELOs; indeed, the only conserved motif in ELOs that is familiar is a LHXXHH histidine box (Fig. 1) that is found in enzymes that carry out

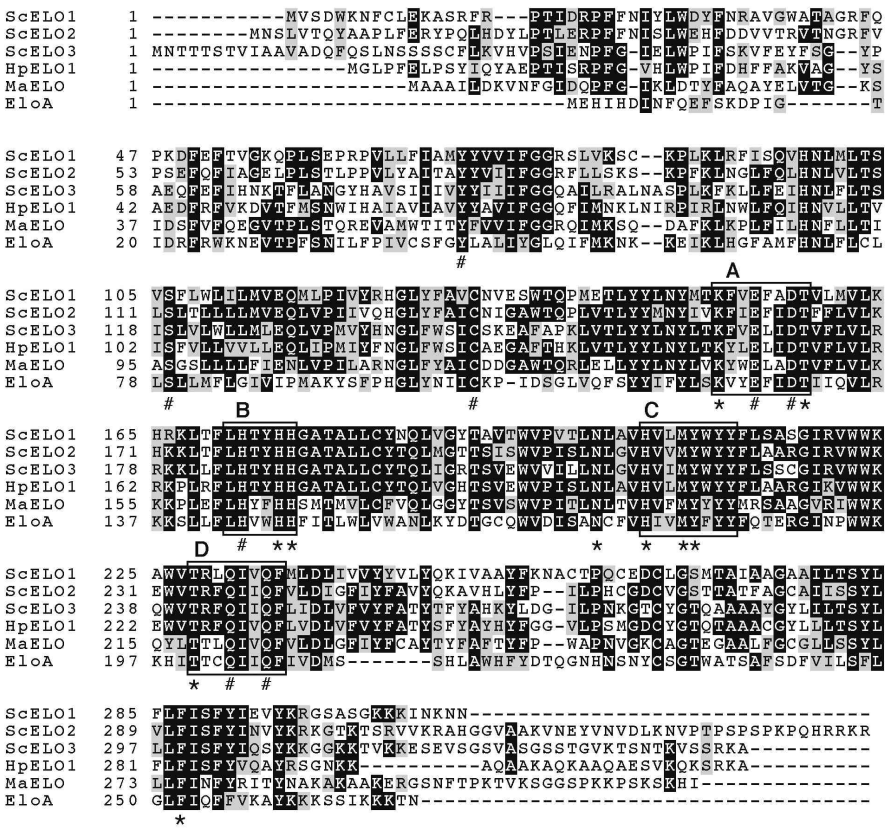

Fig. 1. Multiple sequence alignment of EloA and related fungal ELOs. The four motifs, A–D, found in all members of the ELO family are boxed while residues absolutely (*) or highly conserved (#) in all known ELOs are indicated below the EloA sequence. Gene accession #s: *S. cerevisiae* ScELO1, NP_012339; ScELO2, NP_009963; ScELO3, 013476; *Hansenula polymorpa* HaELO1, AB194620; *Mortierella alpina*, AAF71789; and *D. discoideum*, EloA, EU826171.

oxidative reactions (e.g. fatty acid desaturases), where three or four histidine boxes are thought to bind iron [34]. In addition to the histidine box, four additional conserved motifs that have no similarity to other functionally characterized enzyme families have been identified in the ELO family. The uniqueness of the ELO sequence suggests that these enzymes carry out the condensation reaction using novel chemistry, an understanding of which may impact our understanding and treatment of disease states. Here, we describe the first steps toward understanding the ELO-catalyzed condensation reaction through site-directed mutagenesis of highly conserved amino acids among the ELO family in EloA, a highly active ELO from the cellular slime mold, *D. discoideum*.

2. Materials and methods

2.1. Multiple sequence alignment

Sequences of functionally characterized ELO family members (total of 39 sequences) from mammalian, fungal, algal, fish, protist, and moss sources were aligned and a number of highly conserved residues were identified. The protein multiple sequence alignment was constructed with Clustal X version 1.83.1 using the Gonnet 250 protein weight matrix and default gap parameters followed by bootstrapping with Phylip version 3.65 using the PAM matrix with 1000 replicates and default parameters [35,36].

2.2. Site-directed mutagenesis of EloA

Highly conserved residues in the ELO family were mutated with the QuikChange II Site-Directed Mutagenesis Kit (Stratagene, La Jolla, CA). Forward and reverse primers (Table SI1) were designed to introduce codons for alanine or phenylalanine in place of those for the targeted amino acids. The mutagenesis extension reactions were carried out as described by the manufacturer with EloA subcloned into the *BamHI* and *XhoI* sites of pESc-His (Statagene) as the template. After *DpnI* digestion of the template, mutated plasmids were transformed into XL-1 Blue competent *Escherichia coli* (Stratagene), isolated by Wizard Plus Miniprep DNA kit (Promega, Madison, WI), and sequenced (BigDye® Terminator v3.1 Cycle Sequencing Kit (Applied Biosystems Foster City, CA) with vector-directed primers to confirm installation of the desired mutation.

2.3. Analysis of fatty acid elongation activity

Plasmids encoding wild-type or mutant EloA or the empty vector were transformed into *S. cerevisiae* (InvSc1; Invitrogen) and selected for growth in the absence of histidine on complete minimal media (cm-his) plus 2 g/100 ml dextrose [37]. Starter cultures in rich media were inoculated with a single colony and grown overnight at 30 °C with shaking (250 rpm). Expression cultures were inoculated from starter cultures and grown for 3 days in cm-his with galactose (2 g/100 ml) at 30 °C with shaking (250 rpm). Equivalent cell numbers were collected and fatty acid methyl esters (FAMEs) prepared by transesterification (2% H_2SO_4/MeOH) at 80 °C for 1 h. FAMEs were extracted into hexanes and analyzed by gas chromatography/mass spectrometry (GC/MS) with an Agilent Technologies 7890A GC/5975C MS and HP5 column (J&W Scientific).

2.4. Preparation of microsomes from EloA-expressing yeast

Microsomes were prepared essentially as described [38] from overnight 40-ml expression cultures grown at 30 °C with shaking. Cells were collected and resuspended in isolation buffer (IB; 80 mM Hepes–KOH, pH 7.2; 10 mM KCl, 320 mM sucrose, 5 mM EDTA, 5 mM EGTA, 31 μg/ml benzamidine and 0.1 mM PMSF) and lysed by glass-bead (0.5-mm beads) homogenization on a Bead Beater 8 (BioSpec Products). After unlyzed cells and cell debris were removed, microsomes were pelleted by ultracentrifugation (1 h, 100000×g) and resuspended in IB containing 15% glycerol (2.5 μg total protein/ml).

2.5. Immunoblot analysis of EloA expression

Polyclonal antibodies were raised in a rabbit against a synthesized peptide derived from the EloA amino terminus (residues 1–20; Cocalico Biologicals) and used in immunoblot assays to determine protein levels. Microsomal protein (20 μg) was separated on a 12% SDS–PAGE gel and transferred onto Immobilon-P (Millipore) polyvinylidene fluoride membrane. The blocked membrane (100 mM Tris, pH 7.5, 150 mM NaCl, 0.1% Tween 20) was incubated with anti-EloA (1/500 dilution) combined with anti-Erg27p (1/300 dilution; gift from Martin Bard, Indiana University – Purdue University Indianapolis) for a loading control. The levels of EloA and Erg27p were detected upon incubation with goat-anti rabbit IgG horseradish peroxidase conjugate (Biorad; 1/2500) followed by chemiluminescent detection (Pierce SuperSignal West Pico) with a Biorad photodocumentation system (2 min exposure).

3. Results and discussion

While we have no knowledge of how ELOs catalyze the condensation reaction, we reasoned that highly conserved amino acid residues are likely to have either a structural or a catalytic role in ELO function. A multiple sequence alignment of the functionally characterized ELOs identified four ELO family consensus motifs in EloA as well as a number of additional highly conserved amino acid residues [10]. An alignment of EloA with its closest homologues is presented in Fig.1. Indicated on the sequence alignment are residues that are absolutely (*) or highly (#) conserved among the entire family of functionally characterized ELOs. We targeted absolutely and highly conserved residues found in the ELO family for site-directed mutagenesis and replaced them with alanine or, in the case of tyrosine residues, both alanine and phenylalanine, to interrogate their possible role in EloA structure/function. In all, twenty individual EloA site-directed mutants were prepared in a yeast expression vector and transformed into *S. cerevisiae* for expression and biochemical analysis.

As our activity assay examines the production of $18{:}1^{\Delta 11}$ in vivo and not that of purified enzyme, we examined the level of expression of wild-type and mutant EloA alleles by immunoblot. Microsomes prepared from yeast expressing wild-type EloA and each mutant allele as well as yeast transformed with the empty expression vector (EV) were simultaneously probed with anti-EloA and anti-Erg27p sera. Erg27p is a microsomal protein involved in ergosterol biosynthesis in yeast [39] and was used as a loading control (LC) for total microsomal protein (Fig. 2). As expected, lanes loaded with microsomes derived from yeast transformed with the empty vector showed only a band corresponding to Erg27p (molecular mass = 39.7 kDa), while the lanes loaded with microsomes prepared from yeast expressing wild-type EloA and each mutant had two bands; the LC and EloA (molecular mass = 32.2 kDa).

EloA is a highly active ELO that catalyzes the elongation of $16{:}1^{\Delta 9}$ to $18{:}1^{\Delta 11}$ [10]. The activity of the mutant EloA enzymes was examined upon expression in *S. cerevisiae* through the preparation of FAMEs from total yeast lipids followed by GC/MS analysis and reported as the production of $18{:}1^{\Delta 11}$ relative to wild-type EloA (Fig. 3; for the complete fatty acid profile, see Table SI2). The site-directed mutants fell into three groups based on their activity relative to the wild-type enzyme; those within 10% of

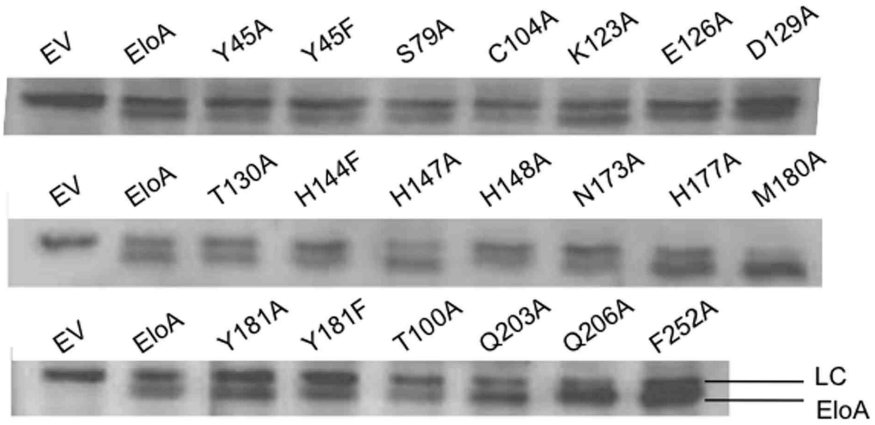

Fig. 2. Immunoblot analysis of microsomes from yeast expressing mutant EloA alleles. Microsomal protein (20 μg) was analyzed by immunoblot with anti-EloA and anti-Erg27. Erg27 (LC) is found in all samples, including the empty vector (EV), while EloA is found only in samples prepared from yeast transformed with wild-type or mutant genes.

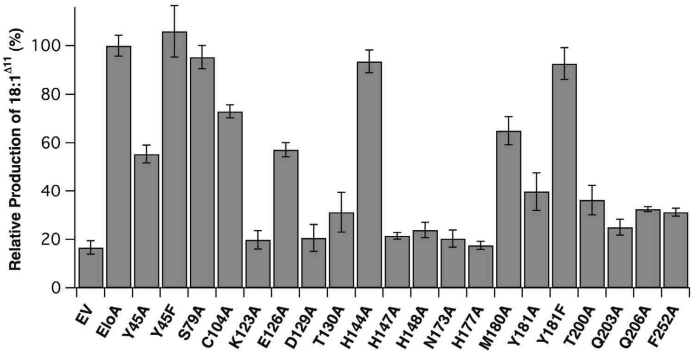

Fig. 3. Production of $18{:}1^{\Delta 11}$ by EloA site-directed mutants. Fatty acid methyl esters prepared from total yeast cellular lipids were analyzed by GC/MS. $18{:}1^{\Delta 11}$, % relative to the wild-type EloA, is presented as the mean ± S.D.; $n = 5$–6. Note that *S. cerevisiae* has a low level of endogenous activity with close to 2% of the total FAMEs as $18{:}1^{\Delta 11}$ (see Table SI2).

wild-type activity (Y45F, S79A, H144A, and Y181F); those with between 35 and 60% of wild-type activity (Y45A, C104A, E126A, M180A, Y181A, T200A); and those with little or no activity (K123A, D129A, T130A, H147A, H148A, N173A, H177A, Q203A, Q206A, and F252A). Each of the mutant EloAs that showed little or no activity, except T130A, H148A, and N173A, demonstrated at least an equivalent level of staining with anti-EloA and a comparable ratio between EloA and LC staining as the wild-type (Fig. 2). This indicates that the absence of EloA activity in yeast expressing these mutant alleles is not the result of the degradation of an unstable polypeptide.

Two of the highly conserved residues in the ELO family, Tyr45 and Tyr181, were replaced with both alanine and phenylalanine residues to probe whether an aromatic ring at these positions was sufficient for a stable and active structure or if the hydroxyl group was required for structure and/or activity. In both cases, the alanine mutant (Y45A and Y181A) demonstrated a dramatically decreased level of activity (55% and 40% of wild-type activity, respectively) while the phenylalanine mutants had within 10% of the wild-type level of activity. As the replacement of each of the tyrosines with phenylalanine resulted in near wild-type activity while the presence of an alanine abrogated activity, it appears that there is a structural requirement for an aromatic ring but no requirement for a phenolic group for catalytic activity at these positions. This result is consistent with the observation that a number of the ELOs without a tyrosine at the position equivalent to Y45 in EloA, have a phenylalanine or tryptophan residue that may play a similar structural role as the tyrosine group.

The cysteine of the Claisen-like condensing enzyme catalytic triad (CHH/N) is essential and is thought to covalently bind the acyl primer prior to condensation with the malonyl-CoA-derived C_2 unit [30,31]. The ELO family does not have an absolutely conserved cysteine residue; C104 of EloA is the only cysteine that is somewhat conserved (30% of sequences) in the family. Mutation of

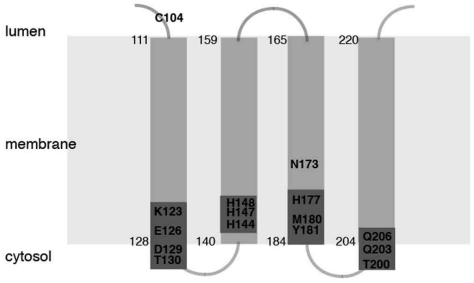

Fig. 4. Topology model of four key membrane-spanning domains of EloA. Residues targeted by site-directed mutagenesis are indicated on a model of the transmembrane topology of EloA [10]. Dark gray boxes indicate four ELO consensus motifs, within which most of the highly conserved residues in ELOs are found.

C104 to alanine resulted in an active enzyme with 73% of the wild-type activity indicating that this residue is not essential for activity. The model for EloA membrane-spanning structure (Fig. 4) [10] predicts that C104 resides in a loop found on the lumenal side of the ER membrane, away from the cytosol where the acyl-CoA and malonyl-CoA substrates of the enzyme are found. Our demonstration that C104 is not essential for activity, along with the model of EloA structure, indicates that this residue does not function in the catalysis of fatty acid elongation and, as there is no other conserved cysteine in the family, ELOs do not appear to covalently bind the acyl primer through a cysteine moiety as seen in the classical Claisen-like condensing enzymes. If the acyl group is covalently bound in the EloA active site, it may be through an ester linkage with a Ser, Thr, or Tyr residue. We found two Thr residues (T130 and T200), proximal to the cytosol, that are important for activity (mutation to alanine resulted in 31% and 36% of wild-type activity, respectively), however the stability of an ester linkage relative to a thiol ester linkage may make the subsequent condensation reaction less likely if the acyl group were bound through a hydroxyl side chain [40]. Alternatively, the acyl primer may not be covalently bound at all, implying that the active site binds two CoA-bound substrates at the same time.

The histidine box (LHXXHH; residues 143–148 in EloA) found in the ELO family is the only primary structural motif found in ELOs with an easily identifiable similarity to other enzymes, those that catalyze oxidative reactions such as the fatty acid desaturases where they are essential and thought to bind the catalytic di-iron center [34]. A variation of the histidine box, where the first histidine is replaced with a glutamine (LQXXHH) is found in "front-end" fatty acid desaturases, such as the Δ^6 desaturase from borage [41] that install double bonds in fatty acids between the carbonyl group and an existing point of unsaturation at the Δ^9 position, and in ELO homologues from *Mortierella alpina* (MALCE1p) and microalgae (*Isochrysis galbana*; IgASE1) [14,42]. We probed the possible role of the conserved residues in the histidine box of EloA and found that mutation of H147 and H148 to alanine each abrogated EloA-catalyzed elongation activity (Fig. 3) but had little effect on the protein level (Fig. 2) while the H144A allele maintained nearly 100% of the wild-type activity. An imidazole group at position 144 is, therefore, not necessary for EloA activity but H147 and H148 are each important for EloA activity, possibly playing roles in catalysis and/or structure. These results are consistent with those reported by Denic and Weismann who found that mutation of the second histidine in the histidine box of *S. cerevisiae* Elo2p (that corresponding to H147 of EloA) to alanine resulted in an inactive enzyme [33]. Mutagenesis of the variant histidine box found in the *I. galbana* IgASE1 ELO [14] where the glutamine residue replacing the first histidine of the canonical histidine box was mutated to either a histidine or an alanine, decreased activity but did not inactivate the enzyme [43] while similar changes in the borage front-end desaturase abrogated activity [41,44]. Together, these results indicate that the histidine box in the ELO family plays a different role than that in the desaturases.

The mutation of many residues that are predicted to reside at the cytosolic side of the ER membrane (Fig. 4) [10,33] from polar residues (K123, D129, N173, H177, Q203, and Q206) to alanine, resulted in the inactivation of EloA (Fig. 3). As the acyl-CoA and malonyl-CoA substrates of the enzyme are found in the cytosol, these results suggest a possible role of these residues in either substrate binding or in catalysis outright. The coenzyme A carrier of the acyl and malonyl groups is negatively charged suggesting that the positively charged residues (K123 and potentially H147, H148, and H177) form salt bridges with the substrate molecules. Interestingly, residues with apparent roles in discriminating among acyl substrates of different lengths are found at the lumen proximal end of ELO transmembrane domains and have been suggested to limit the length of acyl chain accepted by a particular ELO [33,45]. These studies, together with the work we have presented here, strongly suggests that the acyl substrate enters a binding pocket within the membrane-spanning fold of the ELO with the methyl end leading and spanning the membrane while the carboxyl end is held at the cytosolic face where it is available for the condensation reaction with malonyl-CoA.

Our studies have provided insight into residues possibly involved in catalyzing the condensation reaction in ELOs. It appears that the mechanism proceeds by a different pathway than that seen in fatty acid synthases and the related 3-ketoacyl-CoA synthases found in plants and the polyketide synthases. Further studies into the roles of important residues identified here in the condensation reaction are underway.

Acknowledgments

We gratefully acknowledge funding from IUPUI School of Science and Department of Chemistry and Chemical Biology, the gift of antisera raised against Erg27p from Martin Bard, Department of Biology, Indiana University-Purdue University Indianapolis, and constructive conversations with Robert Minto, Department of Chemistry and Chemical Biology, Indiana University-Purdue University Indianapolis. DNA sequencing services were provided by the Miami University Center for Bioinformatics and Functional Genomics.

Appendix A. Supplementary data

Supplementary data associated with this article can be found, in the online version, at http://dx.doi.org/10.1016/j.febslet.2013.10.011.

References

[1] Schweizer, M. (2004) Lipids and Membranes in: Metabolism and Molecular Physiology of *Saccharomyces cerevisiae* (Schweizer, M. and Dickinson, J.R., Eds.), 2nd Ed, pp. 140–223, CRC Press.
[2] Iwabuchi, K., Nakayama, H., Iwahara, C. and Takamori, K. (2010) Significance of glycosphingolipid fatty acid chain length on membrane microdomain-mediated signal transduction. FEBS Lett. 584, 1642–1652.
[3] Schneiter, R., Brugger, B., Amann, C.M., Prestwich, G.D., Epand, R.F., Zellnig, G., Wieland, F.T. and Epand, R.M. (2004) Identification and biophysical characterization of a very-long-chain-fatty-acid-substituted phosphatidylinositol in yeast subcellular membranes. Biochem. J. 381, 941–949.

[4] Samuels, L., Kunst, L. and Jetter, R. (2008) Sealing plant surfaces: cuticular wax formation by epidermal cells. Annu. Rev. Plant Biol. 59, 683–707.

[5] Schreiber, L., Hartmann, K., Skrabs, M. and Zeier, J. (1999) Apoplastic barriers in roots: chemical composition of endodermal and hypodermal cell walls. J. Exp. Bot. 50, 1267–1280.

[6] McMahon, A., Butovich, I.A., Mata, N.L., Klein, M., Ritter, R., Richardson, J., Birch, D.G., Edwards, A.O. and Kedzierski, W. (2007) Retinal pathology and skin barrier defect in mice carrying a Stargardt disease-3 mutation in elongase of very long chain fatty acids-4. Mol. Vis. 13, 258–272.

[7] Qi, B.X., Fraser, T., Mugford, S., Dobson, G., Sayanova, O., Butler, J., Napier, J.A., Stobart, A.K. and Lazarus, C.M. (2004) Production of very long chain polyunsaturated ω-3 and ω-6 fatty acids in plants. Nat. Biotechnol. 22, 739–745.

[8] Haslam, T.M. and Kunst, L. (2013) Extending the story of very-long-chain fatty acid elongation. Plant Sci. 210, 93–107.

[9] Roudier, F., Gissot, L., Beaudoin, F., Haslam, R., Michaelson, L., Marion, J., Molino, D., Lima, A., Bach, L., Morin, H., Tellier, F., Palauqui, J.-C., Bellec, Y., Renne, C., Miquel, M., DaCosta, M., Vignard, J., Rochat, C., Markham, J.E., Moreau, P., Napier, J. and Faurea, J.-D. (2010) Very-long-chain fatty acids are involved in polar auxin transport and developmental patterning in *Arabidopsis*. Plant Cell 22, 364–375.

[10] Blacklock, B.J., Kelley, D. and Patel, S. (2008) A fatty acid elongase ELO with novel activity from *Dictyostelium discoideum*. Biochem. Biophys. Res. Commun. 374, 226–230.

[11] Cameron, D.J., Tong, Z., Yang, Z., Kaminoh, J., Kamiyah, S., Chen, H., Zeng, J., Chen, Y., Luo, L. and Zhang, K. (2007) Essential role of Elovl4 in very long chain fatty acid synthesis, skin permeability barrier function, and neonatal survival. Int. J. Biol. Sci. 3, 111–119.

[12] Oh, C.-S., Toke, D.A., Mandala, S. and Martin, C.E. (1997) *ELO2* and *ELO3*, homologs of the *Saccharomyces cerevisiae ELO1* gene, function in fatty acid elongation and are required for sphingolipid formation. J. Biol. Chem. 272, 17376–17384.

[13] Toke, D.A. and Martin, C.E. (1996) Isolation and characterization of a gene affecting fatty acid elongation in *Saccharomyces cerevisiae*. J. Biol. Chem. 271, 18413–18422.

[14] Qi, B., Beaudoin, F., Fraser, T., Stobart, A.K., Napier, J.A. and Lazarus, C.M. (2002) Identification of a cDNA encoding a novel C18-Δ9 polyunsaturated fatty acid-specific elongating activity from the docosahexaenoic acid (DHA)-producing microalga *Isochrysis galbana*. FEBS Lett. 510, 159–165.

[15] Quist, T.M., Sokolchik, I., Shi, H., Joly, R.J., Bressan, R.A., Maggio, A., Narsimhan, M. and Li, X. (2009) HOS3, an ELO-like gene, inhibits effects of ABA and implicates a S-1-P/ceramide control system for abiotic stress responses in *Arabidopsis thaliana*. Mol. Plant 2, 138–151.

[16] Todd, J., Post-Beittenmiller, D. and Jaworski, J.G. (1999) *KCS1* encodes a fatty acid elongase 3-ketoacyl-CoA synthase affecting wax biosynthesis in *Arabidopsis thaliana*. Plant J. 17, 119–130.

[17] James, D.W., Lim, E., Keller, J., Plooy, I., Ralston, E. and Dooner, H.K. (1995) Directed tagging of the *Arabidopsis* fatty acid elongation1 (*FAE1*) gene with the maize transposon activator. Plant Cell 7, 301–319.

[18] Venkateswari, J., Kanrar, S., Kirti, P.B., Malathi, V.G. and Chopra, V.L. (1999) Molecular cloning and characterization of fatty acid elongation1 (*BjFAE1*) gene of *Brassica juncea*. J. Plant Biochem. Biotechnol. 8, 53–55.

[19] Kim, J., Jung, J.H., Lee, S.B., Go, Y.S., Kim, H.J., Cahoon, R., Markham, J.E., Cahoon, E. and Suh, M.C. (2013) *Arabidopsis* 3-ketoacyl-CoA synthase 9 is involved in the synthesis of tetracosanoic acids as precursors of cuticular waxes, suberins, sphingolipids, and phospholipids. Plant Physiol. 162, 567–580.

[20] Venegas-Caleron, M., Beaudoin, F., Sayanova, O. and Napier, J.A. (2007) Co-transcribed genes for long chain polyunsaturated fatty acid biosynthesis in the protozoon *Perkinsus marinus* include a plant-like 3-ketoacyl coenzyme A synthase. J. Biol. Chem. 282, 2996–3003.

[21] Kajikawa, M., Yamato, K.T., Sakai, Y., Fukuzawa, H., Ohyama, K. and Kohchi, T. (2006) Isolation and functional characterization of fatty acid Δ5-elongase gene from the liverwort *Marchantia polymorpha* L. FEBS Lett. 580, 149–154.

[22] Meyer, A., Kirsch, H., Domergue, F., Abbadi, A., Sperling, P., Bauer, J., Cirpus, P., Zank, T.K., Moreau, H., Roscoe, T.J., Zahringer, U. and Heinz, E. (2004) Novel fatty acid elongases and their use for the reconstitution of docosahexaenoic acid biosynthesis. J. Lipid Res. 45, 1899–1909.

[23] Tehlivets, O., Scheuringer, K. and Kohlwein, S.D. (2007) Fatty acid synthesis and elongation in yeast. Biochim. Biophys. Acta 1771, 255–270.

[24] Zank, T.K., Zahringer, U., Beckmann, C., Pohnert, G., Boland, W., Holtorf, H., Reski, R., Lerchl, J. and Heinz, E. (2002) Cloning and functional characterization of an enzyme involved in the elongation of delta 6-polyunsaturated fatty acids from the moss *Physcomitrella patens*. Plant J. 31, 255–268.

[25] Zhang, K.M., Kniazeva, M., Han, M., Li, W., Yu, Z., Yang, Z., Li, Y., Metzker, M.L., Allikmets, R., Zack, D.J., Kakuk, L.E., Lagali, P.S., Wong, P.W., MacDonald, I.M., Sieving, P.A., Figueroa, D.J., Austin, C.P., Gould, R.J., Ayyagari, R. and Petrukhin, K. (2001) A 5-bp deletion in ELOVL4 is associated with two related forms of autosomal dominant macular dystrophy. Nat. Genet. 27, 89–93.

[26] Raz-Prag, D., Ayyagari, R., Fariss, R.N., Mandal, M.N.A., Vasireddy, V., Majchrzak, S., Webber, A.L., Bush, R.A., Salem, N., Petrukhin, K. and Sieving, P.A. (2006) Haplo insufficiency is not the key mechanism of pathogenesis in a heterozygous *Elovl4* knockout mouse model of STGD3 disease. Invest. Ophthalmol. Vis. Sci. 47, 3603–3611.

[27] Jorgensen, J.A., Zadravec, D. and Jacobsson, A. (2007) Norepinephrine and rosiglitazone synergistically induce Elovl3 expression in brown adipocytes. Am. J. Physiol. Endocrinol. Metab. 293, E1159–E1168.

[28] Zadravec, D., Brolinson, A., Fisher, R.M., Carneheim, C., Csikasz, R.I., Bertrand-Michel, J., Boren, J., Guillou, H., Rudling, M. and Jacobsson, A. (2010) Ablation of the very-long-chain fatty acid elongase ELOVL3 in mice leads to constrained lipid storage and resistance to diet-induced obesity. FASEB J. 24, 4366–4377.

[29] Zadravec, D., Tvrdik, P., Guillou, H., Haslam, R., Kobayashi, T., Napier, J.A., Capecchi, M.R. and Jacobsson, A. (2011) ELOVL2 controls the level of *n*-6 28:5 and 30:5 fatty acids in testis, a prerequisite for male fertility and sperm maturation in mice. J. Lipid Res. 52, 245–255.

[30] Ghanaveti, M. and Jaworski, J.G. (2001) Active-site residues of a plant membrane-bound fatty acid elongase b-ketoacyl-CoA synthase, FAE1 KCS. Biochim. Biophys. Acta 1530, 77–85.

[31] Heath, R.J. and Rock, C.O. (2002) The Claisen condensation in biology. Nat. Prod. Rep. 19, 581–596.

[32] Ghanevati, M. and Jaworski, J.G. (2002) Engineering and mechanistic studies of the *Arabidopsis* FAE1 β-ketoacyl-CoA synthase, FAE1 KCS. Eur. J. Biochem. 269, 3531–3539.

[33] Denic, V. and Weissman, J.S. (2007) A molecular caliper mechanism for determining very long-chain fatty acid length. Cell 130, 663–677.

[34] Shanklin, J., Whittle, E. and Fox, B.G. (1994) Eight histidine residues are catalytically essential in a membrane-associated iron enzyme, stearoyl-CoA desaturase, and are conserved in alkane hydroxylase and xylene monooxygenase. Biochemistry 33, 12787–12794.

[35] Chenna, R., Sugawara, H., Koike, T., Lopez, R., Gibson, T.J., Higgins, D.G. and Thompson, J.D. (2003) Multiple sequence alignment with the clustal series of programs. Nucleic Acids Res. 31, 3497–3500.

[36] Felsenstein, J. (2005) PHYLIP (Phylogeny Inference Package) version 3.6. Distributed by the author, Department of Genome Sciences, University of Washington, Seattle.

[37] Gietz, R.D. and Woods, R.A. (2002) Transformation of yeast by lithium acetate/single-stranded carrier DNA/polyethylene glycol method. Methods Enzymol. 350, 87–96.

[38] Blacklock, B.J. and Jaworski, J.G. (2002) Studies into factors contributing to substrate specificity of membrane-bound 3-ketoacyl-CoA synthases. Eur. J. Biochem. 269, 4789–4798.

[39] Taramino, S., Valachovic, M., Oliaro-Bosso, S., Viola, F., Teske, B., Bard, M. and Balliano, G. (1801) Interactions of oxidosqualene cyclase (Erg7p) with 3-ketoreductase (Erg27p) and other enzymes of sterol biosynthesis in yeast. Biochim. Biophys. Acta 2010, 156–162.

[40] Jencks, W.P., Cordes, S. and Carriuolo, J. (1960) The free energy of thiol ester hydrolysis. J. Biol. Chem. 235, 3608–3614.

[41] Sayanova, O., Smith, M.A., Lapinskas, P., Stobart, A.K., Dobson, G., Christie, W.W., Shewry, P.R. and Napier, J.A. (1997) Expression of a borage desaturase cDNA containing an N-terminal cytochrome *b5* domain results in the accumulation of high levels of Δ6-desaturated fatty acids in transgenic tobacco. Proc. Natl. Acad. Sci. USA 94, 4211–4216.

[42] Sakuradani, E., Nojiri, M., Suzuki, H. and Shimizu, S. (2009) Identification of a novel fatty acid elongase with a wide substrate specificity from arachidonic acid-producing fungus *Mortierella alpina* 1S-4. Appl. Microbiol. Biotechnol. 84, 709–716.

[43] Qi, B., Fraser, T.C.M., Bleakley, C.L., Shaw, E.M., Stobart, A.K. and Lazarus, C.M. (2003) The variant 'His-box' of the C18-Δ9-PUFA-specific elongase IgASE1 from *Isochrysis galbana* is essential for optimum enzyme activity. FEBS Lett. 547, 137–139.

[44] Sayanova, O., Beaudoin, F., Libisch, B., Castel, A., Shewry, P.R. and Napier, J.A. (2001) Mutagenesis and heterologous expression in yeast of a plant Δ6-fatty acid desaturase. J. Exp. Bot. 52, 1581–1585.

[45] Vrinten, P.L., Hoffman, T., Bauer, J. and Qui, X. (2010) Specific protein regions influence substrate specificity and product length in polyunsaturated fatty acid condensing enzymes. Biochemistry 49, 3879–3886.